Check for updates

Global Biogeochemical Cycles

RESEARCH ARTICLE
10.1029/2024GB008256

Special Collection:
Regional Carbon Cycle Assessment and Processes - 2

The Greenhouse Gas Budget of Southeast Asia for 2000–2019 and Pathways Toward Climate Neutrality

Masayuki Kondo[1], Prabir K. Patra[2,3], Josep G. Canadell[4], Philippe Ciais[5], Richard A. Houghton[6], Akihiko Ito[7,8], Chandra S. Deshmukh[9], Tomo'omi Kumagai[7,10,11], Xiangzhong Luo[12,13], Umakant Mishra[14,15], Atul K. Jain[16], Wei Li[17], Gerbrand Koren[18], Stephen Sitch[19], Ben Poulter[20], Hanqin Tian[21], Ana Bastos[22], Ronny Lauerwald[23], Judith A. Rosentreter[24], Naveen Chandra[2], Tazu Saeki[8], Marielle Saunois[5], Ingrid T. Luijkx[25], Takashi Maki[26], Takashi Nakamura[27], Kirari Hirabayashi[28], Takeshi Hirano[29], and Nobuko Saigusa[8]

[1]The IDEC Institute - Center for Peaceful and Sustainable Futures (CEPEAS), Network for Education and Research on Peace and Sustainability (NERPS), Seto Inland Sea Carbon Neutral Research Center (S-CNC), Graduate School of Humanities and Social Sciences International Economic Development Program (IEDP), Graduate School of Innovation and Practice for Smart Society (SmaSo), Hiroshima University, Higashi-Hiroshima, Japan, [2]Research Institute for Global Change, Japan Agency for Marine–Earth Science and Technology (JAMSTEC), Yokohama, Japan, [3]Research Institute for Humanity and Nature (RIHN), Kyoto, Japan, [4]Global Carbon Project, Commonwealth Scientific and Industrial Research Organisation–Environment, Canberra, ACT, Australia, [5]Laboratoire des Sciences du Climat et de l'Environnement, LSCE/IPSL, CEA-CNRS-UVSQ, Université Paris-Saclay, Palaiseau, France, [6]Woodwell Climate Research Center, Falmouth, MA, USA, [7]Graduate School of Agricultural and Life Sciences, The University of Tokyo, Tokyo, Japan, [8]Earth System Division, National Institute for Environmental Studies, Tsukuba, Japan, [9]Asia Pacific Resources International Ltd., Pekanbaru, Indonesia, [10]Institute for Space-Earth Environmental Research, Nagoya University, Nagoya, Japan, [11]Water Resources Research Center, University of Hawai'i at Mānoa, Honolulu, HI, USA, [12]Department of Geography, National University of Singapore, Singapore, Singapore, [13]Center for Nature-based Climate Solutions, Department of Biological Sciences, National University of Singapore, Singapore, Singapore, [14]Computational Biology and Biophysics, Sandia National Laboratories, Livermore, CA, USA, [15]Lawrence Berkeley National Laboratory, Joint BioEnergy Institute, Emeryville, CA, USA, [16]Department of Climate, Meteorology and Atmospheric Sciences, University of Illinois at Urbana–Champaign, Urbana, IL, USA, [17]Department of Earth System Science, Ministry of Education Key Laboratory for Earth System Modeling, Institute for Global Change Studies, Tsinghua University, Beijing, China, [18]Copernicus Institute of Sustainable Development, Utrecht University, Utrecht, The Netherlands, [19]Faculty of Environment, Science and Economy, University of Exeter, Exeter, UK, [20]Spark Climate Solutions, San Francisco, CA, USA, [21]Department of Earth and Environmental Sciences, Center for Earth System Science and Global Sustainability, Schiller Institute for Integrated Science and Society, Boston College, Chestnut Hill, MA, USA, [22]Department of Biogeochemical Integration, Max Planck Institute for Biogeochemistry, Jena, Germany, [23]Université Paris-Saclay, INRAE, AgroParisTech, UMR ECOSYS, Palaiseau, France, [24]Faculty of Science and Engineering, Southern Cross University, Lismore, NSW, Australia, [25]Meteorology and Air Quality Department, Wageningen University and Research, Wageningen, The Netherlands, [26]Meteorological Research Institute, Tsukuba, Japan, [27]Japan Meteorological Agency, Tokyo, Japan, [28]Seto Inland Sea Carbon Neutral Research Center (S-CNC), Hiroshima University, Higashi-Hiroshima, Japan, [29]Research Faculty of Agriculture, Hokkaido University, Sapporo, Japan

Abstract Member countries of the Association of Southeast Asian Nations ratified the Paris Agreement and have initiated their own efforts to reduce greenhouse gas (GHG) emissions. However, the progress of these countries toward climate neutrality remains uncertain. Here, we estimated the combined budget for carbon dioxide (CO_2), methane (CH_4), and nitrous oxide (N_2O) in Southeast Asia for 2000–2019 using bottom-up and top-down approaches. The CO_2 emissions from deforestation were the largest source, followed by anthropogenic fire emissions, which together exceeded the CO_2 uptake by natural vegetation and land-use change legacy (e.g., regrowth), yielding a net source of CO_2 in the biosphere. The region's biosphere was also a net source of CH_4 and N_2O, which, combined with the CO_2 budget, makes the Southeast Asian biosphere a net source of GHGs to the atmosphere, ranging from 2,003.2 ± 406.1 Tg CO_2eq yr^{-1} (bottom-up) to 2,227.5 ± 572.8 Tg CO_2eq yr^{-1} (top-down) for 2000–2019. Among non-biospheric GHG emissions (e.g., fossil fuels and waste-related emissions), coal usage has resulted in an unprecedented increase in CO_2 emissions. The total GHG budget (the biospheric GHG budget plus the non-biospheric GHG fluxes) was calculated as a net source of 3,226.3 ± 406.2 Tg CO_2eq yr^{-1} (bottom-up) and 3,406.4 ± 572.9 Tg CO_2eq yr^{-1} (top-down) for 2000–2019. Our study revealed that Southeast Asia is experiencing the dual challenge of large emissions from

Key Points:

- The greenhouse gas (GHG) budgets (CO_2, CH_4 and N_2O) of Southeast Asia for the 2000–2019 were assessed using top-down and bottom-up approaches
- The GHG budget was a net source to the atmosphere between 3,226 ± 406 Tg CO_2eq yr^{-1} and 3,406 ± 573 Tg CO_2eq yr^{-1}
- Increased GHG emissions from deforestation and coal use during 2000–2019 are obstacles to achieving climate neutrality

Supporting Information:

Supporting Information may be found in the online version of this article.

Correspondence to:

M. Kondo,
redmk92@gmail.com

Citation:

Kondo, M., Patra, P. K., Canadell, J. G., Ciais, P., Houghton, R. A., Ito, A., et al. (2025). The greenhouse gas budget of Southeast Asia for 2000–2019 and pathways toward climate neutrality. *Global Biogeochemical Cycles*, *39*, e2024GB008256. https://doi.org/10.1029/2024GB008256

Received 3 JUN 2024
Accepted 8 SEP 2025

Author Contributions:

Conceptualization: Masayuki Kondo
Data curation: Prabir K. Patra, Richard A. Houghton, Akihiko Ito, Stephen Sitch, Ben Poulter, Hanqin Tian, Ronny Lauerwald, Judith A. Rosentreter, Naveen Chandra, Tazu Saeki, Marielle Saunois, Ingrid T. Luijkx, Takashi Maki, Takashi Nakamura
Formal analysis: Masayuki Kondo
Investigation: Masayuki Kondo
Methodology: Masayuki Kondo
Validation: Masayuki Kondo
Visualization: Masayuki Kondo, Kirari Hirabayashi
Writing – original draft: Masayuki Kondo

© 2025. American Geophysical Union. All Rights Reserved.

Writing – review & editing: Masayuki Kondo, Prabir K. Patra, Josep G. Canadell, Philippe Ciais, Richard A. Houghton, Akihiko Ito, Chandra S. Deshmukh, Tomo'omi Kumagai, Xiangzhong Luo, Umakant Mishra, Atul K. Jain, Wei Li, Gerbrand Koren, Stephen Sitch, Ana Bastos, Ronny Lauerwald, Judith A. Rosentreter, Naveen Chandra, Tazu Saeki, Kirari Hirabayashi, Takeshi Hirano, Nobuko Saigusa

deforestation and coal usage, necessitating the implementation of urgent mitigation strategies to ensure climate neutrality.

Plain Language Summary Southeast Asia is characterized by intense human activities that contribute to increased greenhouse gas (GHG) emissions. To meet the Paris Agreement goals, member countries of the Association of Southeast Asian Nations need to suppress active land-use changes and fossil-fuel usage without compromising economic growth. However, whether a region's GHG budget acts as a net sink or source and the possibility of achieving climate neutrality in the region remain uncertain. Our study is the first to estimate a comprehensive GHG budget for Southeast Asia, encompassing all major natural and anthropogenic sources and sinks of the three major GHGs (CO_2, CH_4, and N_2O) for 2000–2019. The results revealed that the GHG budget in the region was a net source to the atmosphere, with the estimates ranging from 3,226.3 ± 406.2 Tg CO_2eq yr^{-1} to 3,406.4 ± 572.9 Tg CO_2eq yr^{-1}. Land-use changes in forests were a major cause of GHG emissions, followed by fire emissions. GHG emissions from coal usage rapidly increased between the 2000s and the 2010s at a rate that Southeast Asia had never experienced. To achieve climate neutrality, Southeast Asia must develop effective mitigation strategies to manage GHG emissions from land-use changes and coal usage.

1. Introduction

Southeast Asia is a complex geographic region comprising mainland and insular regions dominated by tropical forests, croplands, and savannah woodlands. The forest cover in Southeast Asia constitutes 236 million hectares (Mha), accounting for approximately 15% of the world's tropical forests (Stibig et al., 2014). Renowned as a biodiversity hotspot, the region harbors numerous endemic species; in particular, it hosts the most diverse mangrove species globally (Myers et al., 2000; Richards & Friess, 2015; Sodhi et al., 2004, 2010). The region is also home to extensive tropical peatlands covering an area of 25 Mha (with an estimated carbon pool of 69 Pg C) (Page et al., 2002).

Despite its rich ecosystems, Southeast Asia is one of the regions in the world with the highest rates of deforestation due to land use, land cover change, and forestry (LULUCF), especially the conversion of primary forests to plantations (Achard et al., 2014; Baccini et al., 2017; Mitchard, 2018; Vancutsem et al., 2021; Zeng et al., 2018). Since the early 1980s, due to government policies, the region has experienced rapid major LULUCF changes, such as the opening of large forest areas for transmigration programs in the 1990s and extensive commercial palm oil and rubber production during the 2000s (Murdiyarso et al., 2010; Xu et al., 2022). In recent decades, peat swamp forests have experienced rapid decline due to the expansion of plantations (Carlson et al., 2012, 2018; Hooijer et al., 2012; Miettinen et al., 2016; Page et al., 2002; Wijedasa et al., 2018). In addition, the climate of Southeast Asia is highly susceptible to El Niño–Southern Oscillation (ENSO) (Cai et al., 2019). Notably, synergies between rapid deforestation and ENSO-driven droughts have triggered several extreme episodes of GHG emissions into the atmosphere during fire events in Southeast Asia (Field et al., 2009; Page et al., 2002; van der Werf et al., 2008).

The Association of Southeast Asian Nations (ASEAN) member states ratified the Paris Agreement and initiated their own efforts to reduce greenhouse gas (GHG) emissions. Factors that exacerbate GHG emissions in the region, such as LULUCF activities, ENSO-induced droughts, and continued economic development in the region, must be managed to bring the region's emissions trajectory in line with scenarios stabilizing the climate at 1.5°C or well-below 2°C (Qiu et al., 2024). However, due to the lack of a scientific and integrated assessment of these GHG emissions, the prospects of exceeding the Paris Agreement and achieving climate neutrality (net zero GHG emissions by balancing emissions to be less than or equal to those removed) in Southeast Asia remain highly uncertain.

To support the development of climate neutrality pathways in Southeast Asia, the current state of the region's GHG budget and its evolution in recent decades must be understood. In the current policy environment, wherein such an understanding is sought globally, the second phase of REgional Carbon Cycle Assessment and Processes (RECCAP2), an international initiative of the Global Carbon Project, was implemented to assess the regional GHG budgets of land and ocean (Poulter et al., 2022). To guide this process, RECCAP2 has established a robust

19449224, 2025, 9, Downloaded from https://agupubs.onlinelibrary.wiley.com/doi/10.1029/2024GB008256 by Indian Institute Of Tech - Roorkee, Wiley Online Library on [14/03/2026]. See the Terms and Conditions (https://onlinelibrary.wiley.com/terms-and-conditions) on Wiley Online Library for rules of use; OA articles are governed by the applicable Creative Commons License

framework for regional GHG budget assessments (Ciais et al., 2022). In Southeast Asia, compared to when the carbon dioxide (CO_2) budget was assessed for the first time (Kondo, Ichii, Patra, Canadell, et al., 2018), new CO_2 flux data sets have become available, largely owing to the efforts of RECCAP2, which include data sets for emissions from inland water, estuaries, and coasts (Lauerwald et al., 2023; Rosentreter et al., 2023). In addition, data-driven and process-based estimates of regional methane (CH_4) and nitrous oxide (N_2O) emissions, including those from the industrial, agricultural, and livestock sectors, wetlands, and coastal regions, are widely available (Crippa et al., 2023; McDuffie et al., 2020; Rosentreter et al., 2023; Saunois et al., 2020). This leads to the realization that, for the first time in Southeast Asia, estimates of CO_2, CH_4, and N_2O budgets can be analyzed and managed to meet scientific and climate-policy needs.

As part of RECCAP2, we developed decadal budgets for CO_2, CH_4, and N_2O and combined GHG budgets in Southeast Asia for 2000–2019 with the aim of elucidating the contributions of individual components of natural and anthropogenic origins and the state of the transitions toward climate neutrality. Following the RECCAP2 protocol (Ciais et al., 2022), the GHG budget estimation conducted in this study relied on two independent approaches: top-down estimates of the net GHG flux from atmospheric inversions and bottom-up estimates that integrated the individual components of the GHG budget based on national inventory, modeling, and empirically upscaled observations. Through budget evaluation, we assessed the role of representative anthropogenic activities in the GHG budget (e.g., fossil fuel use, LULUCF, agriculture, and livestock). Furthermore, we illustrate the uncertainties in the approaches used as the basis for budget assessment, with a particular focus on the individual component fluxes that most significantly affected our assessment. Lastly, with the estimated current GHG budgets, we discuss the region's potential for achieving climate neutrality and realizing sustainable development and propose possible pathways for achieving these goals.

2. Materials and Methods

2.1. Study Region

The Southeast Asian region considered for this study comprised 12 countries, including members of the Association of Southeast Asian Nations (ASEAN), Brunei Darussalam, Cambodia, Indonesia, Laos, Malaysia, Myanmar, Singapore, Thailand, Vietnam, and the Philippines, and two non-ASEAN countries, East Timor and Papua New Guinea (PNG) (Figure 1). This definition, based on the regional partitions made for RECCAP2, differs from the United Nations Geoscheme for Southeast Asia, wherein PNG is excluded. For regional delineation, we utilized the National Identifier Grid v4.11 (URL: https://developers.google.com/earth-engine/datasets/catalog/CIESIN_GPWv411_GPW_National_Identifier_Grid).

2.2. Framework of the Greenhouse Gas (GHG) Budget Assessment

In this study, the GHG budget assessment for Southeast Asia was conducted using the bottom-up and top-down approaches outlined in the RECCAP2 protocol by Ciais et al. (2022) (see Figure 2). The bottom-up approach considered individual fluxes within land-freshwater system and emissions embedded in traded products outside the boundaries of Southeast Asia. These fluxes included emissions and sinks from fossil fuel use, waste disposal and burning, geological weathering and seepage, manure management, land vegetation processes, land-use changes in forests, agricultural and natural soil processes, peat decomposition and burning, inland water outgassing from lakes and rivers, and coastal vegetation processes (Figure 2). Additionally, the approach incorporates the lateral transport of carbon through river export and carbon trade via wood and crop products. The top-down approach used in this study was based on the outcomes of atmospheric inversions, which inversely estimated the net GHG flux using modeled atmospheric transport and atmospheric observations of GHGs. The utilization of these approaches in estimating the GHG budget and its components was leveraged based on various independent data sets to assess the robustness of our current understanding of the overall GHG balance and its attributions to independent component fluxes.

2.3. Components of the Bottom-Up CO_2 Budget

2.3.1. Fossil Fuel Emissions: F_{fossil}

Data of CO_2 emissions from fossil fuel usage were obtained from the International Energy Agency (IEA) 2023 (URL: https://www.iea.org/). The IEA 2023 data set encompassed emissions from three major fossil fuel types:

19449224, 2025, 9, Downloaded from https://agupubs.onlinelibrary.wiley.com/doi/10.1029/2024GB008256 by Indian Institute Of Tech - Roorkee, Wiley Online Library on [14/03/2026]. See the Terms and Conditions (https://onlinelibrary.wiley.com/terms-and-conditions) on Wiley Online Library for rules of use; OA articles are governed by the applicable Creative Commons License

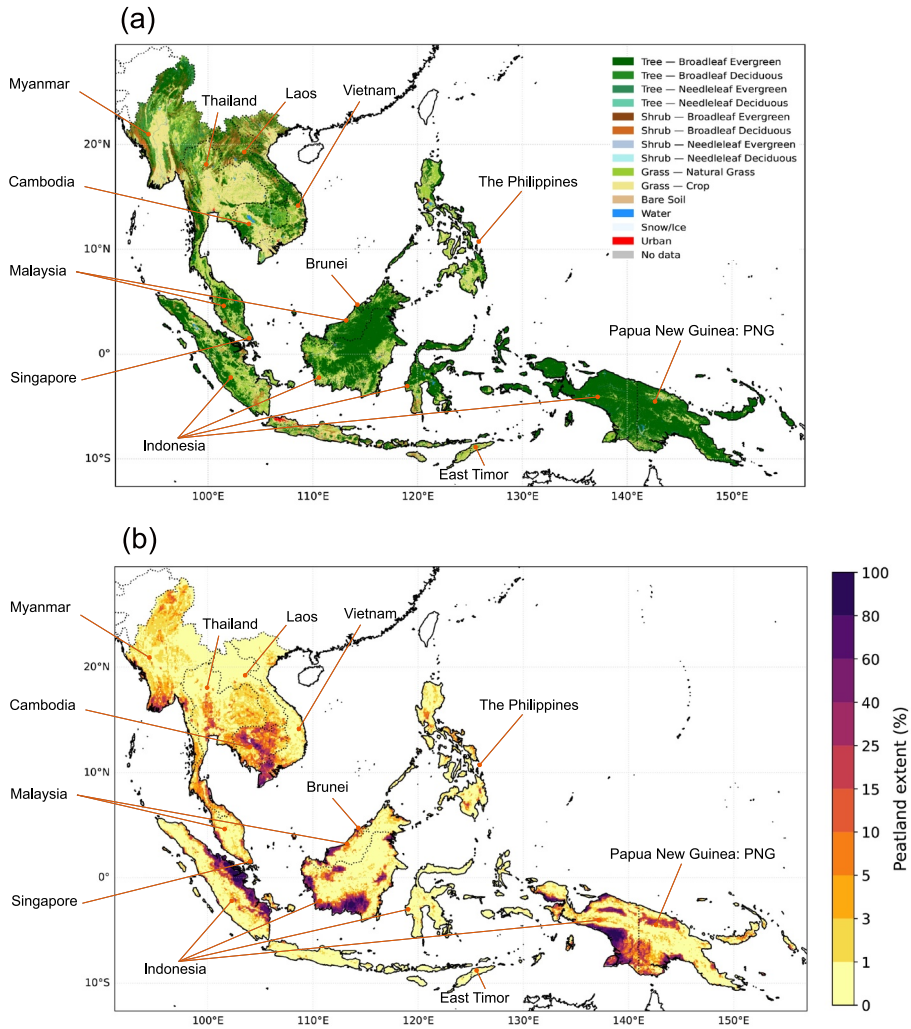


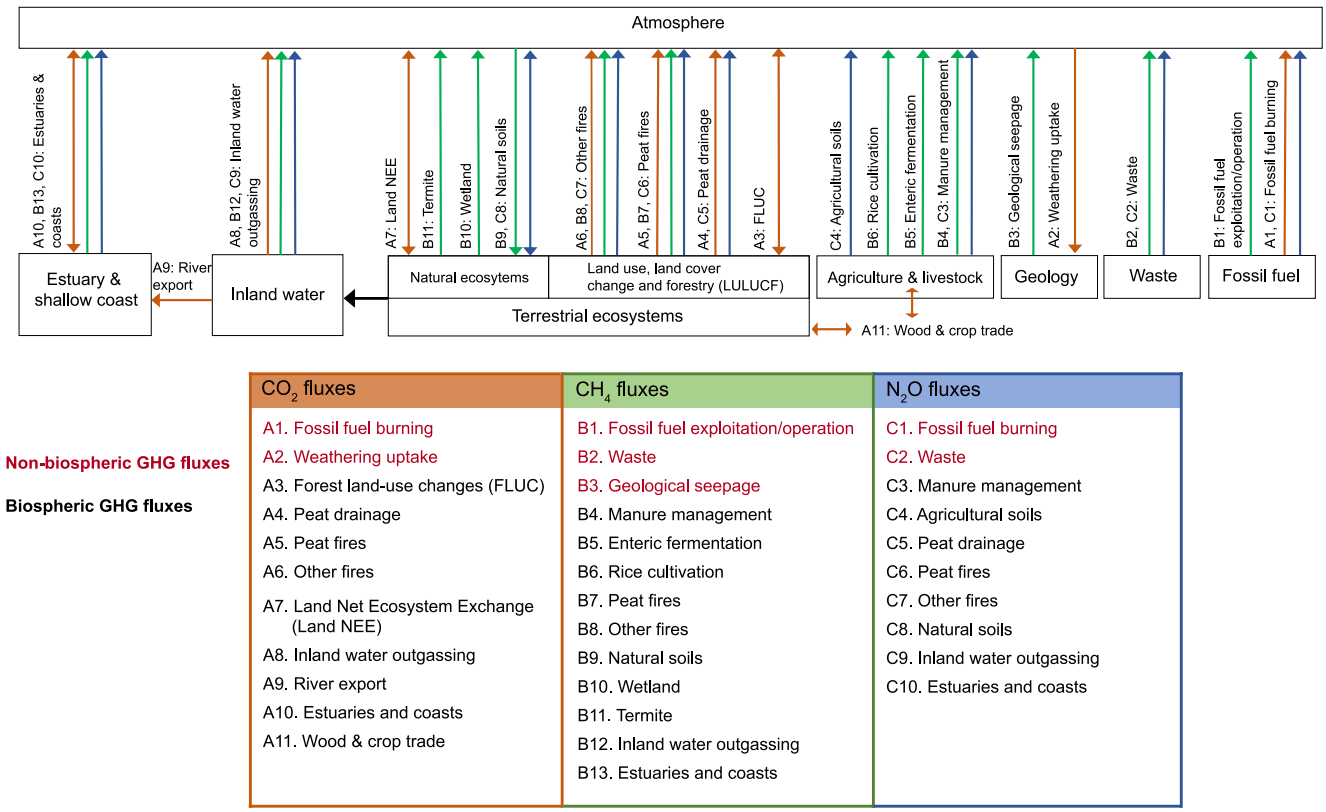
Figure 1. Geolocation of the countries and land-cover types in the Southeast Asian region considered in this study. (a) The map presenting the land cover classification obtained from the European Space Agency-Climate Change Initiative (Li et al., 2018) and (b) the peatland extent based on the global peatland extent created using machine learning (PEAT-ML) (Melton et al., 2022).

oil (crude oil, natural gas liquids, and refinery feedstocks), gas (including natural gas but excluding natural gas liquids), and coal (peat products and oil shale were incorporated in this category). The other two components, emissions from cement production and gas flaring, were obtained from independent sources, Andrew (2018) for emissions from cement production and the British Petroleum Statistical Review of World Energy (URL: https://www.bp.com/en/global/corporate/energy-economics/statistical-review-of-world-energy.html) for emissions from gas flaring, with both accessed from the Global Carbon Budget 2022 (Friedlingstein et al., 2022).

2.3.2. Weathering Uptake: F_{wu}

The data on CO_2 uptake by chemical weathering (F_{wu}) across Southeast Asia were obtained from a spatially explicit estimate of global weathering CO_2 uptake, based on Hartmann et al. (2009). We used the weathering CO_2 uptake model produced by Hartmann et al. (2009), which was based on an enhanced lithological classification scheme comprising a global high-resolution lithology map containing 15 lithology classes. The model was calibrated using a wide range of weathering rates per data set worldwide. According to these data, Southeast Asia is an important hotspot for weathering CO_2 uptake (Figure 2 of Hartmann et al. (2009)).

19449224, 2025, 9, Downloaded from https://agupubs.onlinelibrary.wiley.com/doi/10.1029/2024GB008256 by Indian Institute Of Tech - Roorkee, Wiley Online Library on [14/03/2026]. See the Terms and Conditions (https://onlinelibrary.wiley.com/terms-and-conditions) on Wiley Online Library for rules of use; OA articles are governed by the applicable Creative Commons License



	CO_2 fluxes	CH_4 fluxes	N_2O fluxes
Non-biospheric GHG fluxes	A1. Fossil fuel burning	B1. Fossil fuel exploitation/operation	C1. Fossil fuel burning
	A2. Weathering uptake	B2. Waste	C2. Waste
		B3. Geological seepage	
Biospheric GHG fluxes	A3. Forest land-use changes (FLUC)	B4. Manure management	C3. Manure management
	A4. Peat drainage	B5. Enteric fermentation	C4. Agricultural soils
	A5. Peat fires	B6. Rice cultivation	C5. Peat drainage
	A6. Other fires	B7. Peat fires	C6. Peat fires
	A7. Land Net Ecosystem Exchange (Land NEE)	B8. Other fires	C7. Other fires
	A8. Inland water outgassing	B9. Natural soils	C8. Natural soils
	A9. River export	B10. Wetland	C9. Inland water outgassing
	A10. Estuaries and coasts	B11. Termite	C10. Estuaries and coasts
	A11. Wood & crop trade	B12. Inland water outgassing	
		B13. Estuaries and coasts	

Figure 2. REgional Carbon Cycle Assessment and Processes 2 (RECCAP2) greenhouse gas (GHG) budget assessment framework for Southeast Asia. The carbon dioxide (CO_2), methane (CH_4), and nitrous oxide (N_2O) fluxes are indicated by brown, green, and blue arrows, respectively. In the bottom table, non-biospheric GHG fluxes and biospheric GHG fluxes are shown by red letters and black letters, respectively.

2.3.3. Fluxes From Land Use, Land Cover Change and Forestry (LULUCF)

CO_2 fluxes from LULUCF include CO_2 uptake and release between the terrestrial biosphere and atmosphere that result from deliberate changes in land use and land cover. In this study, we refer to the net change in CO_2 emission resulting from LULUCF as the net LULUCF flux. The net LULUCF flux was calculated by summing the following components: (a) the book-keeping estimates of the gross CO_2 emissions from deforestation and the gross of CO_2 uptake from afforestation, reforestation, and forest regrowth (hereinafter, the fluxes from land-use changes in forests will be referred to as forest land-use change (FLUC) fluxes; see Section 2.3.4); (b) emissions from decomposed peat due to drainage (Section 2.3.5); and (c) emissions from fire, including those from burning peats (Section 2.3.6).

2.3.4. Forest Land-Use Change Flux: F_{FLUC}

The forest land-use change (FLUC) flux (F_{FLUC}) was calculated based on the model employed by Houghton and Castanho (2023), which is an update of Houghton and Nassikas (2017). Hereafter, this model is referred to as the H&C model. H&C is a bookkeeping model that tracks changes in the carbon stored in living and dead vegetation (including wood products) and soil resulting from land-use changes (e.g., deforestation, wood harvesting, crop cultivation, and shifting cultivation). H&C estimated the national-level FLUC fluxes directly based on the national statistics of 5-year changes in the forest area and management stated in the Forest Resources Assessment 2020 report (FAO, 2020), and the annual changes in cropland and pasture area were derived from the Food and Agriculture Organization Corporate Statistical Database (FAOSTAT) (http://www.fao.org/faostat/en/#data). This study evaluated the H&C estimates of the net FLUC flux, gross FLUC emissions and FLUC uptake.

Dynamic global vegetation models and spatially explicit book-keeping models (such as BLUE) (Hansis et al., 2015) are used to estimate FLUC fluxes. However, for Southeast Asia, the inter-decadal variations in their estimates were previously found opposite to those calculated by Houghton and Nassikas (2017) and forest-area

19449224, 2025, 9, Downloaded from https://agupubs.onlinelibrary.wiley.com/doi/10.1029/2024GB008256 by Indian Institute Of Tech - Roorkee, Wiley Online Library on [14/03/2026]. See the Terms and Conditions (https://onlinelibrary.wiley.com/terms-and-conditions) on Wiley Online Library for rules of use; OA articles are governed by the applicable Creative Commons License

19449224, 2025, 9, Downloaded from https://agupubs.onlinelibrary.wiley.com/doi/10.1029/2024GB008256 by Indian Institute Of Tech - Roorkee, Wiley Online Library on [14/03/2026]. See the Terms and Conditions (https://onlinelibrary.wiley.com/terms-and-conditions) on Wiley Online Library for rules of use; OA articles are governed by the applicable Creative Commons License

estimates based on national statistics and satellite observations (Kondo et al., 2022). As described by Kondo et al. (2022), the cause of this discrepancy may be the unrealistic period of peak primary forest loss in Southeast Asia prescribed in the LULUCF forcing data (LUH2 data set) (Chini et al., 2021) used to run these models. Under such circumstances, the N&C model that directly reflects the national statistical data would be the most reliable model to provide FLUC flux estimates for Southeast Asia.

2.3.5. Emissions From Peat Decomposition Due To Drainage: F_{peat_deco}

Drained peatlands present a specific case of CO_2 emissions caused by LULUCF, which is dominated by the loss of soil carbon stock due to the decomposition of dry peat (rather than biomass). CO_2 emissions from peat decomposition due to drainage (F_{peat_deco}) were estimated using two independent data sets. One data set was acquired from Hooijer et al. (2010), who calculated the emissions based on the peatland extents of Sumatra, Kalimantan, and PNG (Wetlands International, 2003, 2004) and the unit area emission factors (EFs) related to peat depths. The other data were acquired from FAOSTAT, and the emissions were calculated using the Tier 1 method of the Intergovernmental Panel on Climate Change (IPCC) Guidelines for National Greenhouse Gas Inventories (IPCC, 2006, 2014), based on the national statistics of the organic soils drained for agriculture and the distribution of histosols.

2.3.6. Fire Emissions From Peat and Other Sources: F_{peat_fire} and F_{other_fire}

In Southeast Asia, CO_2 emissions from fires (F_{peat_fire} and F_{other_fire}) are not of natural origin but anthropogenic; therefore, in this study, we considered this flux as part of the LULUCF flux. The fire emission data were obtained from the Global Fire Emissions Database version 4.1s (GFED4.1s) (van der Werf et al., 2017). GFED4.1s presents an estimation of fire emissions by converting the spatial information regarding fire occurrence, specifically the Moderate Resolution Imaging Spectroradiometer (MODIS) MCD64A1 burnt area (Giglio et al., 2018), into emissions based on the EF, vegetation type, and other ancillary data. GFED4.1s provided the components of fire CO_2 emissions pertaining to grassland, shrubland, and peat fires, which are the dominant fire types in Southeast Asia.

In addition to the GFED4.1s, data pertaining to fire emissions from organic soil in Southeast Asian countries were obtained from FAOSTAT. FAOSTAT provided national-scale fire emission data using the annual burned area data derived from MODIS MCD64A1 (Giglio et al., 2018) and the EFs of peatland fires acquired from the IPCC Wetlands Supplement (IPCC, 2014). Note that the FAOSTAT's "fire emissions from organic soil" data set for Southeast Asia assumed that the emissions were from peat burning.

2.3.7. Natural Ecosystem Carbon Flux: F_{nat_veg}

The carbon flux in natural ecosystems (F_{nat_veg}) in this study is specifically the net ecosystem exchange (NEE). We estimated land NEE in Southeast Asia using an ensemble of 16 Dynamic global vegetation model simulations from the historical carbon cycle model intercomparison project version 10 (TRENDY v10) (Friedlingstein et al., 2022). The TRENDY model simulations spanned the period from the pre-industrial equilibrium (assumed to be at the beginning of the 1700s) to 2020; the simulations were conducted using observation-based forcing data of atmospheric CO_2 and climate. Among the several types of TRENDY v10 simulations, we used the results of simulation S2, which considered variations in CO_2 concentrations and climate. Note that S2 does not consider LULUCF.

2.3.8. River Export Flux: F_{export}

The lateral river transport of carbon to the Southeast Asian coast (F_{export}) was estimated at the river basin scale using the Global Nutrient Export from WaterSheds (NEWS) model framework (Mayorga et al., 2010). The modeled loads of dissolved organic carbon (DOC), dissolved inorganic carbon (DIC), and particulate organic carbon (POC) applied in this study, based on Mayorga et al. (2010) and Hartmann et al. (2009) (for details, refer to Zscheischler et al., 2017), were generated using drivers corresponding to the year 2000, which included the observed hydroclimatological forcing data. Some parameters and observed loads were based on the data from the previous two decades. The adjusted grid-cell-scale exports were aggregated to the basin scale using the NEWS basin definitions (Mayorga et al., 2010) and then reduced by applying the NEWS-based basin-scale consumption water-removal factor acquired from the data on irrigation withdrawals (Mayorga et al., 2010). This study

considered carbon export from rivers as a part of the CO_2 sink, as it was originally a CO_2 sink from the atmosphere into vegetation and ultimately into soils, which is then leached into rivers and transported to the ocean rather than going directly to the atmosphere. This flux has a mixed origin from both natural and anthropogenic sources, which we are unable to partition in this study.

2.3.9. Inland Water Outgassing Flux: $F_{outgassing}$

The river and lake CO_2 outgassing flux ($F_{outgassing}$) data for Southeast Asia were obtained from previous studies compiled by Lauerwald et al. (2023). The metadata contain published values of CO_2 outgassing from lakes and rivers worldwide, which were then broken down into the RECCAP2 land regions. The fluxes were rescaled to consistent estimates of the surface area of lakes, reservoirs (HydroLAKES; Messager et al., 2016) and rivers (Allen & Pavelsky, 2018). For the entire Southeast Asian region, the metadata provided four, five, eight, and five values for CO_2 outgassing from rivers, natural lakes, reservoir lakes, and lakes regulated by dams, respectively.

The four estimates of CO_2 outgassing from rivers varied widely from 161.6 Tg CO_2 yr^{-1} to 2,968.8 Tg CO_2 yr^{-1}; thus, the choice of the representative value (maximum, minimum, median, and average) largely affected the CO_2 budget. The total basin area of the five major river systems in Southeast Asia (the Irrawaddy, Salween, Mekong, Chao Phraya, and Red Rivers) is approximately 1,333,800 km^2, accounting to 16% of the total basin area of the major river system in South America. However, the four estimates of the data set indicated that the maximum estimate of the CO_2 outgassing from rivers in Southeast Asia was as high as 88% of that in South America, followed by 44%, 40%, and 28%. The fact that the rate of CO_2 outgassing from rivers in Southeast Asia is higher than that in South America is not supported by evidence, and a previous study, on which the maximum estimate is based, suggests that the estimate for Southeast Asia may be overestimated because the CO_2 data calculated from the region's pH, alkalinity, and temperature were biased toward high values (Raymond et al., 2013). Therefore, we used the lowest value of the four available estimates for the budget assessment. The mean values were used for the other outgassing estimates (i.e., natural lakes, reservoir lakes, and lakes regulated by dams), as their values did not vary significantly.

2.3.10. Estuarine and Coastal Vegetation Flux: F_{est_coast}

In addition to land CO_2 fluxes, we considered coastal CO_2 fluxes, such as the water-air CO_2 fluxes in estuaries and NEE in coastal wetland ecosystems (F_{est_coast}) (Rosentreter et al., 2023). The data-driven meta-analysis presented by Rosentreter et al. (2023) contains information on three types of estuaries: tidal systems and deltas, lagoons, and fjords (not relevant to Southeast Asia), along with three types of coastal vegetation: mangroves, salt marshes, and seagrass, with the surface area estimated for each coastal type globally. In the coastal meta-analysis, the water-air or NEE flux rates compiled from the literature were averaged over space and time based on the data from each site. The estimated areal flux rates were then grouped for each RECCAP2 region and for each estuary and coastal vegetation type. Finally, non-parametric bootstrapping was performed on the flux rates and the results were scaled to the surface area of each coastal ecosystem type in each RECCAP2 region. Further information on coastal CO_2 flux estimation can be found in Rosentreter et al. (2023). The regional coastal CO_2 flux estimates for Southeast Asia were based on 20 sites for tidal system and delta fluxes and five sites for mangrove NEE; for other coastal ecosystems where less data were available, the global statistics aggregated for the RECCAP2 regions were used (Rosentreter et al., 2023).

2.3.11. Wood and Crop Trade Flux: F_{trade}

We estimated the carbon associated with the export and import of wood and crop products in Southeast Asia (F_{trade}), using the method described by Ciais et al. (2022). Country-based economic data on trade volume and carbon content were obtained from the FAOSTAT for individual wood and crop products. The gross amounts of imported and exported carbon for individual products were estimated using trade volume and carbon content. The total net trade flux for crops and wood was calculated based on the difference between exported and imported carbon estimated in this study. As for river carbon exports, we considered the carbon fluxes resulting in wood and crop trades as part of the CO_2 sink because carbon was exported to or imported from other terrestrial regions, rather than going directly into the atmosphere.

19449224, 2025, 9, Downloaded from https://agupubs.onlinelibrary.wiley.com/doi/10.1029/2024GB008256 by Indian Institute Of Tech - Roorkee, Wiley Online Library on [14/03/2026]. See the Terms and Conditions (https://onlinelibrary.wiley.com/terms-and-conditions) on Wiley Online Library for rules of use; OA articles are governed by the applicable Creative Commons License

19449224, 2025, 9, Downloaded from https://agupubs.onlinelibrary.wiley.com/doi/10.1029/2024GB008256 by Indian Institute Of Tech - Roorkee, Wiley Online Library on [14/03/2026]. See the Terms and Conditions (https://onlinelibrary.wiley.com/terms-and-conditions) on Wiley Online Library for rules of use; OA articles are governed by the applicable Creative Commons License

2.4. Components of the Bottom-Up CH_4 and N_2O Budgets

2.4.1. Emissions From Fossil Fuels and Waste: F_{fossil} and F_{waste} (CH_4 and N_2O)

In this study, the direct anthropogenic emissions of CH_4 and N_2O were the combustion or exploitation of fossil fuels (F_{fossil}) and waste disposal, burning, and wastewater treatment (F_{waste}). Similar to CO_2, CH_4 and N_2O emissions from fossil fuel burning and exploitation in Southeast Asia (F_{fossil}) were primarily sourced from the IEA 2023 data set, including emissions from oil and gaseous fuels as well as emissions from coal mining. For emissions from waste, we employed an ensemble of two global emission inventories: the Community Emissions Data System (CEDS v2021) (McDuffie et al., 2020) and Emissions Database for Global Atmospheric Research (EDGARv7.0) (Crippa et al., 2023).

2.4.2. Geological Seepage Flux: F_{gs} (CH_4)

The data on CH_4 emissions from geological seepage, F_{gs} (the natural degassing of hydrocarbons from the Earth's crust) were obtained from the global gridded data set presented by Etiope et al. (2019). The data set provides information on four types of global seepages: (a) onshore hydrocarbon macro-seeps, including mud volcanoes, (b) submarine (offshore) seeps, (c) diffused micro-seepage, and (d) geothermal manifestations. We extracted these data for Southeast Asia and used a combined value for the CH_4 budget assessment.

2.4.3. Emissions From Livestock and Agriculture: F_{manure}, $F_{enteric}$, and F_{rice} (CH_4), and F_{manure} and $F_{agrisoil}$ (N_2O)

Livestock and agriculture are crucial anthropogenic sources of CH_4 and N_2O emissions. The data for these emissions were derived from an ensemble of three global emission inventories: FAOSTAT, CEDS v2021, and EDGARv7.0. Each inventory encompassed emissions from the common livestock and agricultural sectors necessary for CH_4 and N_2O budget assessments. From these data sets, we estimated CH_4 emissions from manure management (F_{manure}), enteric fermentation ($F_{enteric}$), and rice cultivation (F_{rice}), as well as N_2O emissions from manure management (F_{manure}) and agricultural soils ($F_{agrisoil}$).

2.4.4. Emissions From Peat Decomposition Due To Drainage: F_{peat_deco} (N_2O)

The N_2O emissions from peat decomposition due to drainage (F_{peat_deco}) estimated in this study were based on FAOSTAT (described in Section 2.3.5), which represents the only available estimate.

2.4.5. Fire Emissions: F_{peat_fire} and F_{other_fire} (CH_4 and N_2O)

CH_4 and N_2O emissions from fires encompassing peat burning (F_{peat_fire}) and other types of burning (F_{other_fire}) were obtained from GFED4.1s. As with CO_2, the CH_4 emissions from peat burning were acquired from FAOSTAT, termed "fire emissions from organic soil." FAOSTAT data for emissions from peat burning were not available for N_2O.

2.4.6. Emissions From Wetlands: F_{wet} (CH_4)

CH_4 emissions from wetlands (F_{wet}) were estimated using an ensemble of 13 process-based model simulations previously prepared for the Global Methane Budget (Saunois et al., 2020). These models calculated CH_4 emissions as the product of the emission flux density and methane-producing surface extent. All models were forced by common data sets, such as the reconstructed climate fields (CRU-JRA) and the remote sensing-based dynamical wetland area data set (Wetland Area Dynamics for Methane Modeling: WAD2M).

2.4.7. Oxidative Consumption by and Emissions From Natural Soils: F_{soil} (CH_4 and N_2O)

A process-based model simulation from Vegetation Integrated SImulator for Trace gases (VISIT) (Ito et al., 2023) was used to quantify the oxidative consumption of atmospheric CH_4 by natural soils (F_{soil}). VISIT calculates CH_4 transfer from the atmosphere to the soil base using a semi-empirical scheme (Curry, 2007) embedded within the model, which parameterizes soil airspace gas diffusivity using an empirical equation for soil temperature and moisture content. Microbial oxidation activity was also calculated using the simulated soil temperature and moisture content. Following Curry (2007), VISIT assumes that the cropland fraction affects the soil oxidation rate, while considering the effect of nitrogen fertilizers on the reduction of CH_4 oxidation rates.

N_2O emissions from natural soils (F_{soil}) were obtained from seven process-based model simulations of the Global N_2O Model Intercomparison Project (NMIP) (Tian et al., 2018, 2020). From the seven available simulations (S0–S6), we used S2, which considers the spatiotemporal effects of climate, atmospheric CO_2, LULUCF, nitrogen deposition, and fertilizer. However, this simulation did not consider the effects of manure management.

2.4.8. Emissions From Termite Activity: $F_{termite}$ (CH_4)

CH_4 emissions from termite activity ($F_{termite}$) were obtained from process-based model simulations conducted using VISIT (Ito, 2023). The simulation of CH_4 emissions was based on prescribed global data sets of field-observed termite colonies, calculated as the product of termite biomass density and EFs. Termite biomass was estimated using a regression model that represented the dependence on gross primary productivity.

2.4.9. Inland Water Outgassing: $F_{outgassing}$ (CH_4 and N_2O)

Similar to CO_2, the data for river and lake CH_4 and N_2O outgassing ($F_{outgassing}$) in Southeast Asia were obtained from the data sets compiled by Lauerwald et al. (2023).

2.4.10. Estuarine and Coastal Vegetation Fluxes: F_{est_coast} (CH_4 and N_2O)

Data for CH_4 and N_2O fluxes from estuarine and coastal vegetation (F_{est_coast}) in Southeast Asia were obtained from a meta-analysis by Rosentreter et al. (2023). In Southeast Asia, the analysis included 11 sites for tidal systems and delta CH_4 fluxes and 11 sites for mangrove CH_4 fluxes. The available N_2O data for Southeast Asia include eight tidal systems and delta sites. All other coastal ecosystem GHG fluxes in Southeast Asia were estimated based on global statistics (Rosentreter et al., 2023).

2.5. Top-Down Approach

Atmospheric inversions or top-down analyses provide estimates of the net CO_2 flux at the surface resulting from all fluxes between the biosphere and atmosphere. In this study, we estimated the net CO_2 flux using nine atmospheric inverse frameworks: ACTM_CONTRAIL (Saeki & Patra, 2017), CAMS (Chevallier et al., 2010), Carbon-Tracker CT2022 (Peters et al., 2007), Carbon-Tracker-Europe (van der Laan-Luijkx et al., 2017), CMS-flux (Liu et al., 2021), JMA2021 (Maki et al., 2023), GOSAT L4A (Maksyutov et al., 2013), MIROC4-ACTM (Chandra et al., 2022), and UoE (Feng et al., 2016). In situ surface observations of atmospheric CO_2 over Southeast Asia are limited, and most atmospheric inversions have been carried out without constraints provided by direct CO_2 measurements in the region. Therefore, the magnitude and trend of the net CO_2 flux in the region depend on the performance of the constraints in the nearby regions. Two models (ACTM_CONTRAIL and JMA2021) used CO_2 observations from the upper troposphere obtained by Japan Airlines (JAL) at cruising altitudes between Tokyo and Sydney/Brisbane (Comprehensive Observation Network for TRace gases by AIrLiner: CONTRAIL, Matsueda et al., 2008; Machida et al., 2008). One model (GOSAT L4A) uses column-averaged CO_2 observations acquired by the GOSAT satellite (Yoshida et al., 2013) as a constraint.

The net CH_4 flux was based on ten CH_4 inversion systems obtained from the Global Methane Budget (Saunois et al., 2020). These inversions were based on tower CH_4 observations and/or column-averaged CH_4 observations acquired by the GOSAT satellite. The inversion models used in this study were Carbon-Tracker-Europe (Tsuruta et al., 2017), GELCA (Ishizawa et al., 2016), LMDz-PYVAR (Zheng, Chevallier, Ciais, Yin, & Wang, 2018; Zheng, Chevallier, Ciais, Yin, Deeter et al., 2018), MIROC4-ACTM (Chandra et al., 2021; Patra et al., 2016, 2018), NICAM-TM (Niwa, Tomita, et al., 2017; Niwa, Fujii, et al., 2017), NIES-TM, NIES-TM-FLEXPART (Maksyutov et al., 2021; Wang et al., 2019), TM5-CAMS (Pandey et al., 2016; Segers & Houwelling, 2018), TM5-4DVAR (Bergamaschi et al., 2013), and TOMCAT (McNorton et al., 2018).

We estimated the net N_2O flux using four independent N_2O inversion systems described by Tian et al. (2020). These models included GEOS-Chem (Wells et al., 2015), INVICAT (Wilson et al., 2014), MIROC4-ACTM (Patra et al., 2018), and PyVAR_CAMS (Thompson et al., 2014). Unlike the inversion models used for CO_2 and CH_4 inversions, none of the four N_2O inversion systems was constrained by atmospheric N_2O measurements (e.g., aircraft or satellites) over Southeast Asia. Therefore, the accuracy of top-down N_2O budgets for Southeast Asia may be limited.

19449224, 2025, 9, Downloaded from https://agupubs.onlinelibrary.wiley.com/doi/10.1029/2024GB008256 by Indian Institute Of Tech - Roorkee, Wiley Online Library on [14/03/2026]. See the Terms and Conditions (https://onlinelibrary.wiley.com/terms-and-conditions) on Wiley Online Library for rules of use; OA articles are governed by the applicable Creative Commons License

2.6. Budget Assessment

In this study, we estimated two types of GHG budgets: the biospheric GHG budget (accounting for only the fluxes in and out of the biosphere) and the total GHG budget (including non-biospheric fluxes, i.e., emissions due to the extraction and use of fossil fuels, waste disposal and burning, and geological fluxes, such as chemical weathering and geological seepage). The biospheric bottom-up (BU) and top-down (TD) CO_2, CH_4, and N_2O budgets are constructed as follows:

$$\text{Biospheric BU}_{CO_2} = F_{FLUC} + F_{peat_deco} + F_{peat_fire} + F_{other_fire} + F_{nat_veg} + F_{outgassing} + F_{export} + F_{est_coast} + F_{trade} \quad (1)$$

$$\text{Biospheric BU}_{CH_4} = F_{manure} + F_{enteric} + F_{rice} + F_{peat_fire} + F_{other_fire} + F_{wet} + F_{termite} + F_{outgassing} + F_{est_coast} \quad (2)$$

$$\text{Biospheric BU}_{N2_O} = F_{manure} + F_{agrisoil} + F_{peat_deco} + F_{peat_fire} + F_{other_fire} + F_{soil} + F_{outgassing} + F_{est_coast} \quad (3)$$

The results of atmospheric inversions cannot be directly compared with bottom-up estimates due to the difference in components included in net flux estimates (Kondo et al., 2020). Therefore, lateral CO_2 fluxes, such as river carbon transport and wood and crop trade, were added to the net CO_2 flux estimated by atmospheric inversions so that both the top-down and bottom-up approaches accounted for the same fluxes in the CO_2 budgets (Ciais et al., 2022; Kondo et al., 2020). With the necessary adjustments, the biospheric top-down CO_2, CH_4, and N_2O budgets (excluding non-biospheric GHG fluxes) can be represented as follows:

$$\text{Biospheric TD}_{CO_2} = CO_2 \text{ inversion} - F_{export} - F_{trade} \quad (4)$$

$$\text{Biospheric TD}_{CH_4} = CH_4 \text{ inversion} \quad (5)$$

$$\text{Biospheric TD}_{N_2O} = N_2O \text{ inversion} \quad (6)$$

Using the biospheric GHG budgets, the total GHG budgets were calculated by adding the non-biospheric components, as follows:

$$\text{Total BU}_{CO_2} = \text{Biospheric BU}_{CO_2} + F_{fossil} + F_{wu} \quad (7)$$

$$\text{Total BU}_{CH_4} = \text{Biospheric BU}_{CH_4} + F_{fossil} + F_{waste} + F_{gs} \quad (8)$$

$$\text{Total BU}_{N_2O} = \text{Biospheric BU}_{N_2O} + F_{fossil} + F_{waste} \quad (9)$$

$$\text{Total TD}_{CO_2} = \text{Biospheric TD}_{CO_2} + F_{fossil} + F_{wu} \quad (10)$$

$$\text{Total TD}_{CH_4} = \text{Biospheric TD}_{CH_4} + F_{fossil} + F_{waste} + F_{gs} \quad (11)$$

$$\text{Total TD}_{N_2O} = \text{Biospheric TD}_{N_2O} + F_{fossil} + F_{waste} \quad (12)$$

Finally, the total impact of the three GHGs on global warming (in terms of CO_2 equivalent: CO_2eq) was calculated for the bottom-up and top-down approaches using the global warming potentials over a 100-year time horizon (GWP100). Following the guidelines in IPCC AR6 (Canadell et al., 2021; Forster et al., 2021), we used a GWP100 value of 27.0 for non-fossil fuel CH_4 budget components, such as the emissions of biogenetic origin ($GWP_{CH4\text{-}NFF}$), 29.8 for fossil fuel fugitive CH_4 emissions ($GWP_{CH4\text{-}FF}$), and 273 for the N_2O budget (GWP_{N2O}). The integrated GHG budgets for the three gases are calculated as follows:

$$\text{GHG budget} = [CO_2] + [CH_4 - \text{fossil fuel}] \times [GWP_{CH_4-FF}] + [CH_4 - \text{non fossil fuel}] \times [GWP_{CH_4-NFF}] + [N_2O] \times GWP_{N_2O} \quad (13)$$

19449224, 2025, 9, Downloaded from https://agupubs.onlinelibrary.wiley.com/doi/10.1029/2024GB008256 by Indian Institute Of Tech - Roorkee, Wiley Online Library on [14/03/2026]. See the Terms and Conditions (https://onlinelibrary.wiley.com/terms-and-conditions) on Wiley Online Library for rules of use; OA articles are governed by the applicable Creative Commons License

19449224, 2025, 9, Downloaded from https://agupubs.onlinelibrary.wiley.com/doi/10.1029/2024GB008256 by Indian Institute Of Tech - Roorkee, Wiley Online Library on [14/03/2026]. See the Terms and Conditions (https://onlinelibrary.wiley.com/terms-and-conditions) on Wiley Online Library for rules of use; OA articles are governed by the applicable Creative Commons License

Table 1
Carbon Dioxide (CO_2) Budget and Its Components (Tg CO_2 yr^{-1}) for Southeast Asia in the 2000s (2000–2009), the 2010s (2010–2019), and 2000–2019

Category	Components	2000s	2010s	2000–2019
Direct human emissions	Oil, gas, and coal	815.1	1,208.4	1,011.7
	Cement production	62.2	103.0	82.6
	Gas flaring	11.9	13.1	12.5
Geology	Weathering uptake	−124.7	−124.7	−124.7
LULUCF fluxes	Gross FLUC emissions	1,824.9	2,078.4	1,951.7
	Gross FLUC uptake	−1,086.4	−1,143.7	−1,115.0
	Peat decomposition due to drainage	268.0	302.8	285.4
	Peat burning	178.0 ± 45.5	176.0 ± 51.1	192.6 ± 48.3
	Biomass burning excluding peat burning	775.8	648.8	712.3
Natural land fluxes	Vegetation carbon flux (land NEE)	−1,210.4 ± 277.9	−1,175.5 ± 300.0	−1,193.0 ± 288.9
Inland water fluxes	River export: DOC	−88.0	−88.0	−88.0
	River export: DIC	−183.3	−183.3	−183.3
	River export: POC	−113.7	−113.7	−113.7
	Outgassing from lakes and rivers	177.5	177.5	177.5
Estuarine fluxes	Tidal system, deltas, and lagoons	11.9	11.9	11.9
Coastal vegetation fluxes	Mangrove, salt marsh, and seagrasses	−178.7	−178.7	−178.7
Trade	Woods and crop	−122.0	−151.9	−137.0
Budget	Type	2000s	2010s	2000–2019
Biospheric CO_2 budget	Bottom-up	253.6 ± 281.6	360.7 ± 304.3	308.1 ± 292.9
	Top-down	539.5 ± 344.6	683.2 ± 690.4	611.3 ± 517.5
Total CO_2 budget	Bottom-up	1,018.0 ± 281.6	1,560.5 ± 304.3	1,289.3 ± 292.9
	Top-down	1,303.9 ± 344.6	1,883.0 ± 690.4	1,593.5 ± 517.5

Note. Land use, land cover change and forestry (LULUCF); Forest land-use changes (FLUC); Net ecosystem exchange (NEE); Dissolved organic carbon (DOC); Dissolved inorganic carbon (DIC); Particulate organic carbon (POC).

2.7. Uncertainty

The uncertainty of the GHG budget could not be precisely defined because of the absence of the physical uncertainty associated with each component flux. We could only estimate statistical uncertainty; achieving highly accurate uncertainty estimations was challenging due to the limited data availability for the region. In cases where multiple estimates were accessible for a component flux, a standard deviation of 1σ was considered after thoroughly scrutinizing the estimates. However, the majority of the component fluxes lacked sufficient multiple estimates to derive a statistically meaningful spread, often providing only one estimate. Therefore, in this budget assessment, we estimated the uncertainty of the GHG budget using the error propagation method while considering the standard deviations of 1σ from the component fluxes with more than two independent estimates (i.e., $\delta\mathrm{GHG} = \sqrt{(\delta\mathrm{comp1})^2 + (\delta\mathrm{comp2})^2 + (\delta\mathrm{comp3})^2 \ldots}$, where δGHG is the uncertainty of the CO_2 budget, and δcomp is the 1σ standard deviation for a component flux).

3. Greenhouse Gas (GHG) Budget of Southeast Asia

3.1. CO_2 Budget

Table 1 presents the components of the CO_2 budget for the 2000s, the 2010s, and 2000–2019. The land NEE (CO_2 exchange in natural ecosystems) showed the largest CO_2 sink, amounting to −1,193.0 ± 288.9 Tg CO_2 yr^{-1} for 2000–2019, closely followed by the gross FLUC uptake (i.e., CO_2 uptake from reforestation and regrowth: at −1,115.0 Tg CO_2 yr^{-1}). These two components contributed to 40% and 37% of the total gross biospheric CO_2 uptake in Southeast Asia, respectively. Lateral carbon fluxes, such as river exports and wood and crop trade,

19449224, 2025, 9, Downloaded from https://agupubs.onlinelibrary.wiley.com/doi/10.1029/2024GB008256 by Indian Institute Of Tech - Roorkee, Wiley Online Library on [14/03/2026]. See the Terms and Conditions (https://onlinelibrary.wiley.com/terms-and-conditions) on Wiley Online Library for rules of use; OA articles are governed by the applicable Creative Commons License

constitute 18% of gross CO_2 uptake, indicating a large amount of carbon transport to the coasts of Southeast Asia and to the ocean. Coastal ecosystems, including mangrove forests, represent the smallest proportion at 6% of the total gross biospheric CO_2 uptake.

Over the two decades, the gross FLUC emissions (i.e., emissions directly resulting from deforestation, degradation, and wood harvesting) was the most significant emission component, amounting to 1,951.7 Tg CO_2 yr^{-1} (Table 1). This accounts for 59% of the total gross CO_2 emissions from the biosphere, followed by fire emissions (27%), in which peat fires account for 5%, and the other types of fires account for 22%. The remaining components accounted for smaller proportions, for example, emissions from peat decomposition (11%) and inland water outgassing (7%). Although Southeast Asia is home to peatlands, peat-related CO_2 emissions (peat decomposition and peat burning) comprise 24% of the gross FLUC emissions, signifying the greater impact of deforestation in the region. The gross FLUC emissions surpassed the gross FLUC uptake, resulting in a net CO_2 source (from FLUC) of 836.6 Tg CO_2 yr^{-1}. Consequently, the LULUCF flux (the sum of the gross FLUC emissions and uptake, peat drainage, peat fires, and other types of fires) in Southeast Asia collectively represented large net sources of CO_2, amounting to 2,011.3 Tg CO_2 yr^{-1}.

The biospheric CO_2 budget from the bottom-up approach represented a net source of 253.6 ± 292.9 Tg CO_2 yr^{-1} for 2000–2019 (Table 1). This budget reflects the impact of FLUC and fire emissions, canceling and exceeding the two major gross sink components (i.e., land NEE and gross FLUC uptake). Biospheric CO_2 budget estimates obtained using the top-down approach were comparable to those using the bottom-up approach, indicating a net source of 611.3 ± 517.5 Tg CO_2 yr^{-1} (Table 1). The CO_2 budgets from both approaches increased by approximately 100 Tg CO_2 yr^{-1} from the 2000s to the 2010s, with increasing emissions from gross FLUC emissions contributing the most among all components.

For 2000–2019, the non-biospheric CO_2 emissions were dominated by emissions from oil, gas, and coal burning (1,011.7 Tg CO_2 yr^{-1}), followed by those from cement production (82.6 Tg CO_2 yr^{-1}) and gas flaring (12.5 Tg CO_2 yr^{-1}) (Table 1). These emissions increased substantially from the 2000s to the 2010s, with a 48% increase in emissions from oil, gas, and coal, 66% in emissions from cement production, and 11% in emissions from gas flaring. The weathering CO_2 uptake was −124.7 Tg CO_2 yr^{-1}, which canceled 11% of the CO_2 emissions from fossil fuels. The sum of these fossil fuel emissions and weathering uptake amounted to 982.1 Tg CO_2 yr^{-1} during 2000–2019. This results in the total CO_2 budget (sum of the biospheric CO_2 budget and the non-biospheric CO_2 fluxes) being a net source of 1,289.3 ± 292.9 Tg CO_2 yr^{-1} in the bottom-up approach and 1,593.5 ± 517.5 Tg CO_2 yr^{-1} in the top-down approach. The increase in the total CO_2 budgets from the 2000s to the 2010s (ranging from 542.48 to 579.10 Tg CO_2 yr^{-1}) was approximately five times greater than the increase in the biospheric CO_2 budgets and was driven by rising emissions from the combustion of oil, natural gas, and coal (Table 1).

3.2. CH_4 Budget

As shown in Table 2, in the 2000s and the 2010s, all components of the CH_4 budget, except for natural soils, were net sources of CH_4 to the atmosphere. Among all the components, wetland (19.1 ± 7.50 Tg CH_4 yr^{-1}) dominated the CH_4 emissions of Southeast Asia for 2000–2019, followed by rice cultivation (8.90 ± 0.21 Tg CH_4 yr^{-1}). These two components accounted for 49% and 23% of the total CH_4 emissions from the biosphere, respectively. Other components, including emissions from enteric fermentation, fires, and termites, showed roughly equivalent magnitudes, with each contributing less than 10% of the total emissions. Oxidative consumption by natural soils was solely a net sink of the atmospheric CH_4, amounting to −2.42 Tg CH_4 yr^{-1} in 2000–2019, canceling 6% of the total CH_4 emissions from the biosphere.

The biospheric CH_4 budget from the bottom-up approach indicated a net source of 36.2 ± 7.53 Tg CH_4 yr^{-1} in 2000–2019 (Table 2). The top-down approach yielded a relatively consistent estimate of 46.4 ± 7.60 Tg CH_4 yr^{-1} (Table 2). The budget estimated using the two approaches showed a moderate increase between the 2000s and the 2010s (1.5 Tg CH_4 yr^{-1} in the bottom-up approach and 5.3 Tg CH_4 yr^{-1} in the top-down approach), reflecting that the components of CH_4 emissions from the biosphere have not undergone rapid changes during these decades. This differs from the notable increase in emissions from in the region indicated by a process-based model study reported by Ito et al. (2023).

Regarding fossil fuels, oil and gaseous fuel extraction and coal mining were the largest CH_4 emitters in 2000–2019 (2.46 Tg CH_4 yr^{-1} and 2.22 Tg CH_4 yr^{-1}, respectively), followed by waste disposal, waste burning, and

19449224, 2025, 9, Downloaded from https://agupubs.onlinelibrary.wiley.com/doi/10.1029/2024GB008256 by Indian Institute Of Tech - Roorkee, Wiley Online Library on [14/03/2026]. See the Terms and Conditions (https://onlinelibrary.wiley.com/terms-and-conditions) on Wiley Online Library for rules of use; OA articles are governed by the applicable Creative Commons License

Table 2
Methane (CH_4) Budget (and Its Components) (Tg CH_4 yr^{-1}) for Southeast Asia in the 2000s (2000–2009), the 2010s (2010–2019), and 2000–2019

Category	Components	2000s	2010s	2000–2019
Direct human emissions	Oil and gas extraction	2.38	2.53	2.46
	Coal mining	1.33	3.11	2.22
	Waste disposal, waste burning, and waste-water treatment	1.29 ± 0.34	1.78 ± 0.29	1.54 ± 0.32
Geology	Geological seepage	1.49	1.49	1.49
Agriculture/Livestock	Manure management	0.38 ± 0.28	0.47 ± 0.35	0.42 ± 0.32
	Enteric fermentation	3.11 ± 0.03	3.45 ± 0.02	3.28 ± 0.02
	Rice cultivation	8.60 ± 0.11	9.20 ± 0.30	8.90 ± 0.21
LULUCF fluxes	Peat burning	2.21 ± 0.45	2.13 ± 0.36	2.17 ± 0.40
	Biomass burning excluding peat burning	0.67	0.56	0.62
Natural land fluxes	Wetland	18.9 ± 7.43	19.3 ± 7.57	19.1 ± 7.50
	Natural soils	−2.36	−2.49	−2.42
	Termites	1.12	1.17	1.15
Inland water fluxes	Outgassing from lakes and rivers	2.90	2.90	2.90
Estuarine fluxes	Tidal system, deltas, and lagoons	0.004	0.004	0.004
Coastal vegetation fluxes	Mangrove, salt marsh, and seagrasses	0.068	0.068	0.068
Budget	Type	2000s	2010s	2000–2019
Biospheric CH_4 budget	Bottom-up	35.6 ± 7.45	36.7 ± 7.60	36.2 ± 7.53
	Top-down	43.8 ± 7.11	49.1 ± 8.10	46.4 ± 7.60
Total CH_4 budget	Bottom-up	42.1 ± 7.46	45.6 ± 7.60	43.9 ± 7.53
	Top-down	50.3 ± 7.12	58.0 ± 8.10	54.1 ± 7.61

Note. Land use, land cover change and forestry (LULUCF).

wastewater treatment (1.54 ± 0.32 Tg CH_4 yr^{-1}) (Table 2). Similar to CO_2 emissions from fossil fuel use, CH_4 emissions from fossil fuel extraction (particularly from coal mining) increased more than two-folds between the 2000s and the 2010s. Geological seepage yielded CH_4 emissions of 1.49 Tg CH_4 yr^{-1}, equivalent to waste-related CH_4 emissions. However, the sum of fossil fuel and geological CH_4 emissions (7.70 Tg CH_4 yr^{-1}) remained significantly smaller than the emissions from wetlands (Table 2). Consequently, the non-biospheric emissions only contributed modestly to the total CH_4 budget (sum of the biospheric CH_4 budget and non-biospheric emissions): 43.9 ± 7.53 Tg CH_4 yr^{-1} in the bottom-up approach and 54.1 ± 7.61 Tg CH_4 yr^{-1} in the top-down approach. The total CH_4 budgets increased between the 2000s and the 2010s, with a rate greater than the biospheric CH_4 budgets (3.6 Tg CH_4 yr^{-1} in the bottom-up approach and 7.7 Tg CH_4 yr^{-1} in the top-down approach), largely due to the increased emissions from coal mining (Table 2).

3.3. N_2O Budget

Table 3 outlines the components of the N_2O budget for the 2000s, the 2010s, and 2000–2019. Among all components, emissions from natural soils were the largest (1.93 ± 0.68 Tg N_2O yr^{-1} for 2000–2019), constituting a dominant proportion (73%) of the total N_2O emissions from the biosphere. This was followed by the agricultural soils (12%), with the remaining components contributing smaller proportions. Although emissions were relatively small, manure management, agricultural soils, and peat decomposition showed a 12%–21% increase in N_2O emissions from the 2000s to the 2010s.

The biospheric N_2O budget from the bottom-up approach indicated a net source of 2.64 ± 0.71 Tg N_2O yr^{-1} in 2000–2019 (Table 3). The top-down approach estimates were approximately half of the bottom-up estimates, at 1.33 ± 0.49 Tg N_2O yr^{-1}. Despite a common increase in budget estimates between the 2000s and the 2010s, the bottom-up estimate showed a small increase (~5%), whereas the top-down approach showed an increase four times larger (~20%).

19449224, 2025, 9, Downloaded from https://agupubs.onlinelibrary.wiley.com/doi/10.1029/2024GB008256 by Indian Institute Of Tech - Roorkee, Wiley Online Library on [14/03/2026]. See the Terms and Conditions (https://onlinelibrary.wiley.com/terms-and-conditions) on Wiley Online Library for rules of use; OA articles are governed by the applicable Creative Commons License

Table 3
Nitrous Oxide (N_2O) Budget (and Its Components) (Tg N_2O yr^{-1}) for Southeast Asia in the 2000s (2000–2009), the 2010s (2010–2019), and 2000–2019

Category	Components	2000s	2010s	2000–2019
Direct human emissions	Oil and gas	0.020	0.032	0.026
	Waste disposal, waste burning, and waste-water treatment	0.041 ± 0.028	0.053 ± 0.036	0.047 ± 0.032
Agriculture/Livestock	Manure management	0.13 ± 0.14	0.14 ± 0.15	0.13 ± 0.15
	Agricultural soils	0.30 ± 0.18	0.36 ± 0.23	0.33 ± 0.20
LULUCF fluxes	Peat decomposition due to drainage	0.17	0.19	0.18
	Peat burning	0.18	0.18	0.18
	Biomass burning excluding peat burning	0.029	0.024	0.026
Natural land fluxes	Natural soils	1.92 ± 0.66	1.94 ± 0.67	1.93 ± 0.68
Inland water fluxes	Outgassing from lakes and rivers	0.015	0.015	0.015
Estuarine fluxes	Tidal system, deltas, and lagoons	0.005	0.005	0.005
Coastal vegetation fluxes	Mangrove, salt marsh, and seagrasses	0.002	0.002	0.002
Budget	Type	2000s	2010s	2000–2019
Biospheric N_2O budget	Bottom-up	2.58 ± 0.70	2.70 ± 0.73	2.64 ± 0.71
	Top-down	1.21 ± 0.41	1.45 ± 0.57	1.33 ± 0.49
Total N_2O budget	Bottom-up	2.64 ± 0.70	2.78 ± 0.73	2.71 ± 0.71
	Top-down	1.41 ± 0.41	1.67 ± 0.57	1.54 ± 0.49

Note. Land use, land cover change and forestry (LULUCF).

For 2000–2019, despite a significant increase between the 2000s and the 2010s, the non-biospheric N_2O emissions from oil and gaseous fuel burning (0.026 Tg N_2O yr^{-1}) and waste disposal and burning (0.047 ± 0.032 Tg N_2O yr^{-1}) were significantly smaller than biospheric N_2O emissions, such as those from natural soils, agricultural soils, and manure management (Table 3) Consequently, those non-biospheric emissions contributed only modestly to the total N_2O budget (sum of the biospheric N_2O budget and non-biospheric emissions): 2.71 ± 0.71 Tg N_2O yr^{-1} in the bottom-up approach and 1.54 ± 0.49 Tg N_2O yr^{-1} in the top-down approach. The total N_2O budgets of both approaches increased between the 2000s and the 2010s with rates similar to those in the biospheric N_2O budgets (Table 3).

3.4. GHG Budget

For 2000–2019, the total biospheric GHG budget assessment (sum of the biospheric CO_2, CH_4, and N_2O budgets) revealed that the net contribution of Southeast Asia to the atmosphere was 2,003.2 ± 406.1 Tg CO_2eq yr^{-1} (based on the bottom-up approach) and 2,227.5 ± 572.8 Tg CO_2eq yr^{-1} (based on the top-down approach), respectively (Table 4). In both, the top-down and bottom-up approaches, all the individual budgets indicated that the region's biosphere was a net source of GHGs to the atmosphere, where in terms of the global warming potential, the biospheric CH_4 budget was the largest (bottom-up: 976.0 ± 203.2 Tg CO_2eq yr^{-1}; top-down: 1,253.1 ± 205.3 Tg CO_2eq yr^{-1}), followed by the biospheric N_2O budgets (bottom-up: 720.0 ± 194.5 Tg CO_2eq yr^{-1}; top-down: 363.1 ± 134.8 Tg CO_2eq yr^{-1}) and the biospheric CO_2 budgets (bottom-up: 308.1 ± 292.9 Tg CO_2eq yr^{-1}; top-down: 611.3 ± 517.5 Tg CO_2eq yr^{-1}), over the past two decades (Tables 4). The biospheric GHG budget increased toward a net source of 9% in the bottom-up estimate and 17% in the top-down estimate between the 2000s and the 2010s. This increase over the decades was common in all budgets and was most significant in the biospheric CO_2 budgets (bottom-up: 42%; top-down: 27%).

For 2000–2019, the total GHG budget of Southeast Asia, inclusive of non-biospheric GHG emissions from fossil fuels, waste, weathering uptake, and geological seepages, was calculated to be 3,226.3 ± 406.2 Tg CO_2eq yr^{-1} (bottom-up approach) and 3,406.4 ± 572.9 Tg CO_2eq yr^{-1} (top-down approach). In terms of the CO_2 equivalent, for 2000–2019, the non-biospheric CH_4 and N_2O emissions amounted to 185.1 and 19.90 Tg CO_2eq yr^{-1}, respectively, moderately increasing the net source of biospheric CH_4 and N_2O budgets by a maximum of 21% (Tables 2 and 3). During the same period, non-biospheric CO_2 emissions amounted to 1,107.0 Tg CO_2 yr^{-1}

19449224, 2025, 9, Downloaded from https://agupubs.onlinelibrary.wiley.com/doi/10.1029/2024GB008256 by Indian Institute Of Tech - Roorkee, Wiley Online Library on [14/03/2026]. See the Terms and Conditions (https://onlinelibrary.wiley.com/terms-and-conditions) on Wiley Online Library for rules of use; OA articles are governed by the applicable Creative Commons License

Table 4
Bottom-Up and Top-Down Carbon Dioxide (CO_2), Methane (CH_4), Nitrous Oxide (N_2O), and Total Greenhouse Gas (GHG) Budget Estimates (Tg CO_2eq yr^{-1}) for Southeast Asia for the 2000s (2000–2009) and the 2010s (2010–2019) and 2000–2019

Budget	Approach type	2000s	2010s	2000–2019	Changes from the 2000s to the 2010s (%)
Biospheric CO_2 budget	Bottom-up	253.6 ± 281.6	360.7 ± 304.3	308.1 ± 292.9	42
	Top-down	539.5 ± 344.6	683.2 ± 690.4	611.3 ± 517.5	27
Total CO_2 budget	Bottom-up	1,018.0 ± 281.6	1,560.5 ± 304.3	1,289.3 ± 292.9	53
	Top-down	1,303.9 ± 344.6	1,883.0 ± 690.4	1,593.5 ± 517.5	44
Biospheric CH_4 budget	Bottom-up	960.6 ± 201.3	991.5 ± 205.1	976.0 ± 203.2	3
	Top-down	1,181.7 ± 192.0	1,324.5 ± 218.6	1,253.1 ± 205.3	12
Total CH_4 budget	Bottom-up	1,146.2 ± 201.5	1,248.0 ± 205.3	1,197.1 ± 203.4	9
	Top-down	1,292.4 ± 192.2	1,492.6 ± 218.8	1,392.5 ± 205.5	15
Biospheric N_2O budget	Bottom-up	703.9 ± 190.6	736.1 ± 198.3	720.0 ± 194.5	5
	Top-down	330.3 ± 112.9	395.9 ± 156. 7	363.1 ± 134.8	20
Total N_2O budget	Bottom-up	720.5 ± 190.6	759.3 ± 198.3	739.9 ± 194.5	5
	Top-down	384.9 ± 112.9	455.9 ± 156.7	420.4 ± 134.8	18
Biospheric GHG budget	Bottom-up	1,918.7 ± 395.1	2,088.3 ± 417.2	2,003.2 ± 406.1	9
	Top-down	2,051.5 ± 410.3	2,403.5 ± 740.9	2,227.5 ± 572.8	17
Total GHG budget	Bottom-up	2,884.7 ± 395.2	3,567.9 ± 417.2	3,226.3 ± 406.2	24
	Top-down	2,981.2 ± 410.4	3,831.5 ± 741.0	3,406.4 ± 572.9	29

(Table 1), increasing the net source of the biospheric CO_2 budget by a maximum of four times. The increase in fossil fuel emissions facilitated almost all individual total budgets of CO_2, CH_4, and N_2O toward a net source between the 2000s and the 2010s, compared with those of the biospheric budgets (Table 4).

4. GHG Emissions of Anthropogenic Origin

Our GHG budget assessment revealed that Southeast Asia was a large net source of GHGs during 2000–2019, and the net source substantially increased between the 2000s and the 2010s, which makes achieving climate neutrality challenging for the region. As GHG emissions of anthropogenic origin are largely responsible for the region's total GHG budget being a net source of GHG (Tables 1–3), reducing and managing these emissions at low levels is a core part of planning a climate-neutral pathway in the region. Effective future reduction plans require a deep understanding of anthropogenic GHG emissions, assessed under two categories: those that originate in the biosphere, such as land-use changes, peat drainage, fires, agriculture, and livestock, and direct emissions from human activities, such as fossil fuel emissions and waste disposal and burning.

4.1. Anthropogenic GHG Emissions in the Biosphere

A comparison of anthropogenic CO_2, CH_4, and N_2O emissions in the biosphere revealed that gross FLUC emissions were the dominant component, exceeding other anthropogenic GHG emissions in the terms of warming potential (Figures 3a and 3b), highlighting the major effects of land-use changes on GHG emissions in Southeast Asia. CO_2 emissions from fires, including those from peat burning, were the 2nd largest GHG emission source, followed by CO_2 emissions from peat decomposition. The relative importance of these top three GHG emitters remained unchanged between the 2000s and the 2010s (Figures 3a and 3b). Among all CH_4-inducing anthropogenic activities considered in this study (e.g., agriculture, livestock, and fires), rice cultivation was the largest CH_4 emitter for the 2000s and the 2010s (Figures 3a and 3b) accounting for only 12% of the warming potential of the gross FLUC emissions. The dominant component of anthropogenic N_2O emissions, that is, agricultural soils, had a relatively small contribution to the warming potential during the 1990s and the 2010s, accounting for less than 5% of the gross FLUC emissions (Figures 3a and 3b).

Focusing on the top three anthropogenic GHG emitters in the biosphere (CO_2 emissions from FLUC, fires, and peat decomposition), we found that a large proportion of these emissions was concentrated in Indonesia among the nine major Southeast Asian countries evaluated (Figures 3c and 3d). In the 2000s and the 2010s, Indonesia

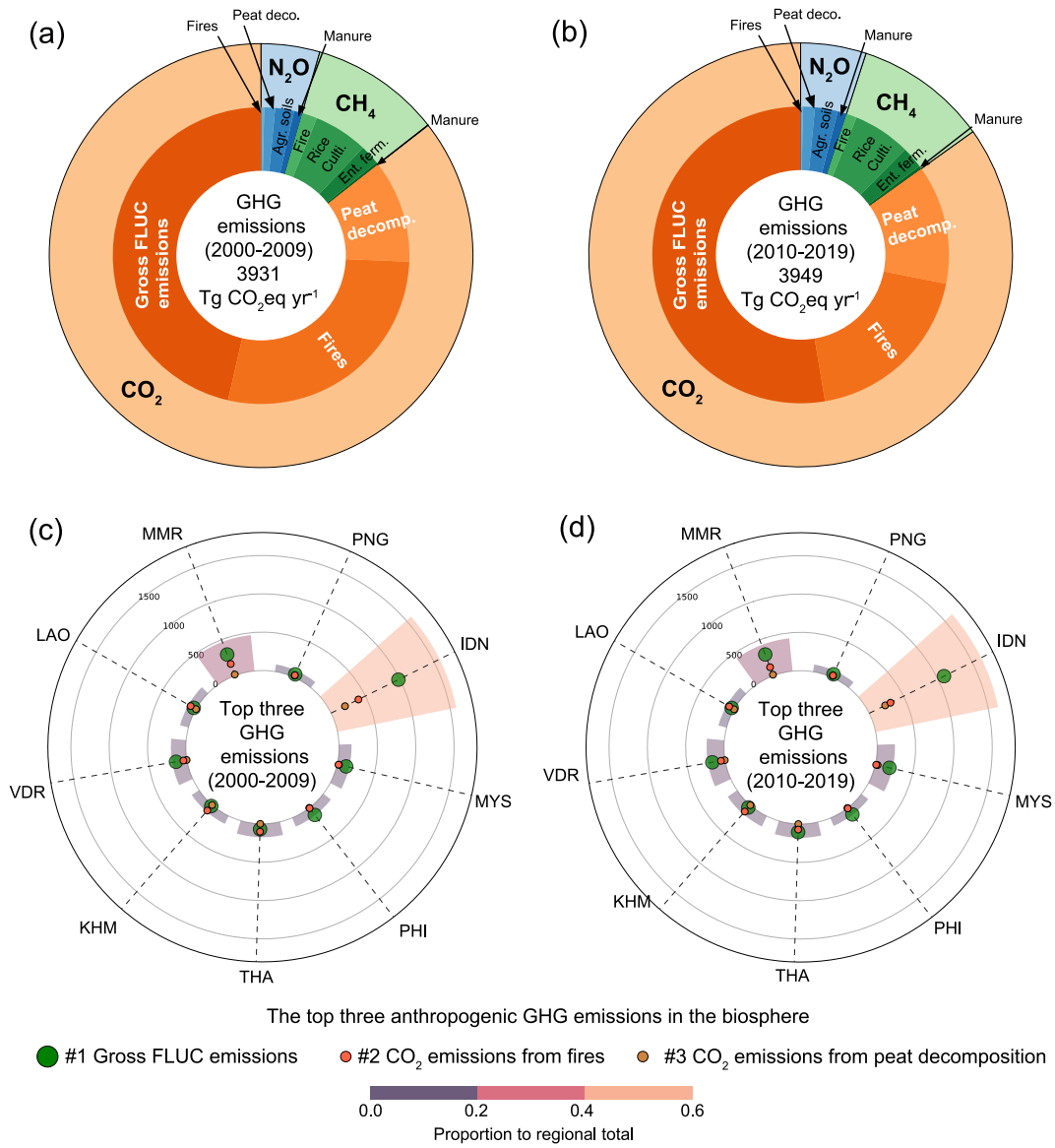


Figure 3. Decadal carbon dioxide (CO_2), methane (CH_4), and nitrous oxide (N_2O) emissions resulting from land use, land cover change and forestry (LULUCF), agriculture, and livestock. The proportions of anthropogenic greenhouse gas (GHG) emissions in the biosphere accounted for by CO_2, CH_4, and N_2O (outer circle) and their components (inner circle) are shown for (a) the 2000s and (b) the 2010s. "Fire" is the sum of emissions from peat fires and other types of fires. Proportions of the top three anthropogenic GHG emissions (gross forest land-use change (FLUC) emissions, CO_2 emissions from fires, and CO_2 emissions from peat decomposition) of the nine major Southeast Asian countries for (c) the 2000s and (d) the 2010s. The bars represent the proportion of each county to the regional total of the summed top three anthropogenic GHG emissions. Circles represent the proportion of each county to the regional total of the top three anthropogenic GHG emissions (green, gross FLUC emissions; red, CO_2 emissions from fires; and brown; CO_2 emissions from peat decomposition). Three letter country codes following ISO 3166-1 were used: Myanmar (MMR), Laos (LAO), Vietnam (VDR), Cambodia (KHM), Thailand (THA), the Philippines (PHI), Malaysia (MYS), and Indonesia (IND).

alone accounted for approximately 52% of these emissions in Southeast Asia, followed by Myanmar (~14%), and the rest of the countries contributed less than 10%. These proportions remained relatively unchanged between the 2000s and the 2010s. In these periods, gross FLUC emissions were the largest emissions in many countries, including Indonesia, Myanmar, Vietnam, Malaysia, Thailand (only in the 2010s), and the Philippines. Fire emissions were the largest in some continental countries, including Laos, Cambodia, and Thailand (only in the 2000s).

19449224, 2025, 9, Downloaded from https://agupubs.onlinelibrary.wiley.com/doi/10.1029/2024GB008256 by Indian Institute Of Tech - Roorkee, Wiley Online Library on [14/03/2026]. See the Terms and Conditions (https://onlinelibrary.wiley.com/terms-and-conditions) on Wiley Online Library for rules of use; OA articles are governed by the applicable Creative Commons License

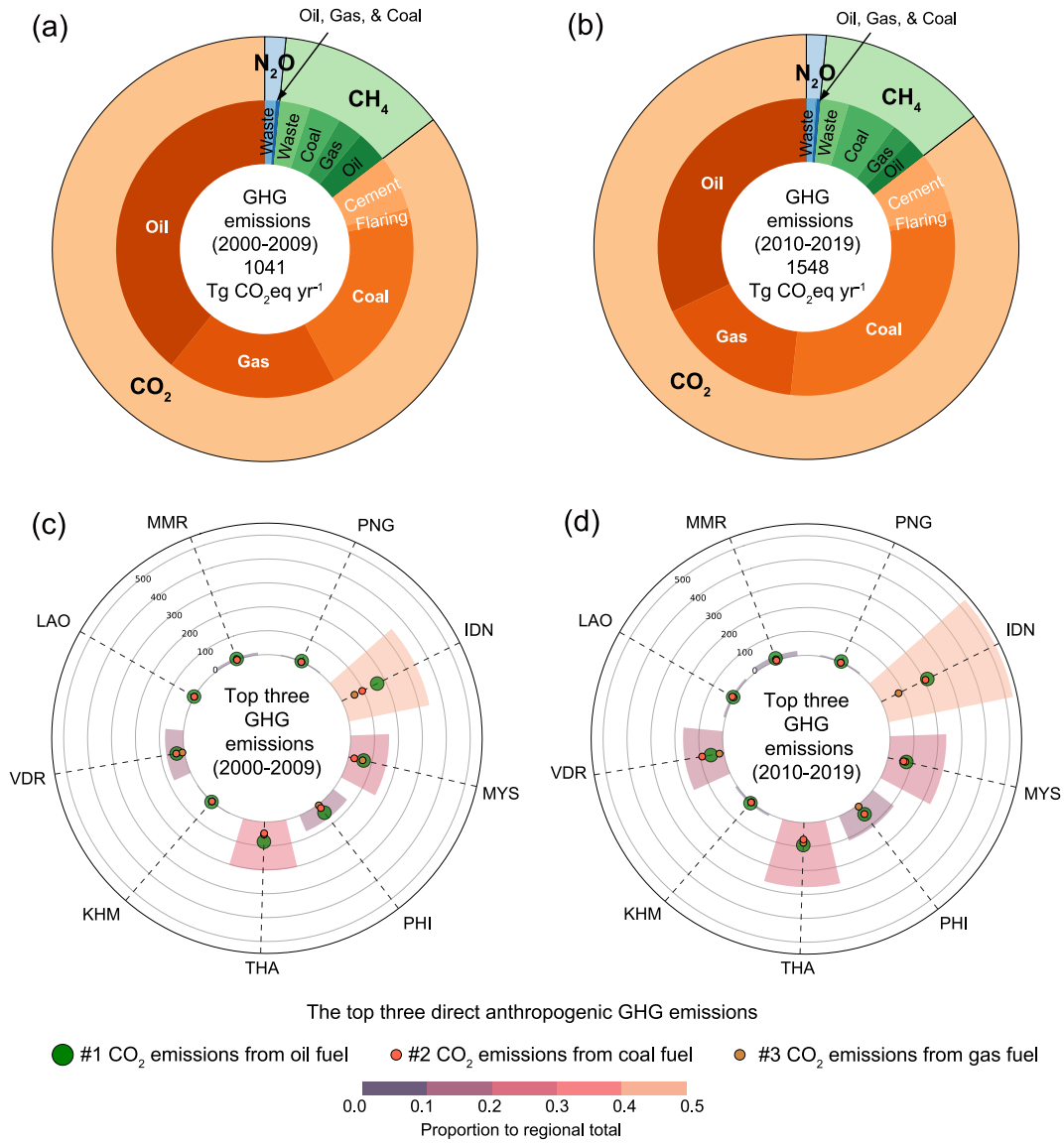


Figure 4. Decadal carbon dioxide (CO_2), methane (CH_4), and nitrous oxide (N_2O) emissions resulting from fossil fuel burning, exploitation, mining, and waste. The proportions of direct anthropogenic greenhouse gas (GHG) emissions accounted for by CO_2, CH_4, and N_2O (outer circle) and their components (inner circle) are shown for (a) the 2000s and (b) the 2010s. Proportions of the top three direct anthropogenic CO_2 emissions (CO_2 emissions from oil, coal, and gas fuels) of the nine major Southeast Asian countries for (c) the 2000s and (d) the 2010s. The bars represent the proportion of each county to the regional total of the summed top three direst anthropogenic CO_2 emissions. Circles represent the proportion of each county to the regional total of the top three direct anthropogenic CO_2 emissions (green, CO_2 emissions from oil fuels; red, CO_2 emissions from coal fuels; and brown; CO_2 emissions from gas fuels). Three letter country codes following ISO 3166-1 were used: Myanmar (MMR), Laos (LAO), Vietnam (VDR), Cambodia (KHM), Thailand (THA), the Philippines (PHI), Malaysia (MYS), and Indonesia (IND).

4.2. GHG Emissions From Fossil Fuels and Waste

Among all the GHG emissions from fossil fuels and waste in the region, CO_2 emissions from oil fuels were a major component in the 2000s, accounting for 40%, followed by CO_2 emissions from coal fuels (21%), and gas fuels (19%) (Figure 4a). The order of the top three GHG emitters did not change between the 2000s and the 2010s, but the proportion of CO_2 emissions from coal fuels in the total CO_2 emissions increased to 30%, whereas those of oil and gas fuels were reduced to 32% and 16%, respectively (Figures 4a and 4b). In the 2000s, CH_4 emissions from oil extraction, coal mining, and waste accounted for equivalent proportions (~26%) of the total

19449224, 2025, 9, Downloaded from https://agupubs.onlinelibrary.wiley.com/doi/10.1029/2024GB008256 by Indian Institute Of Tech - Roorkee, Wiley Online Library on [14/03/2026]. See the Terms and Conditions (https://onlinelibrary.wiley.com/terms-and-conditions) on Wiley Online Library for rules of use; OA articles are governed by the applicable Creative Commons License

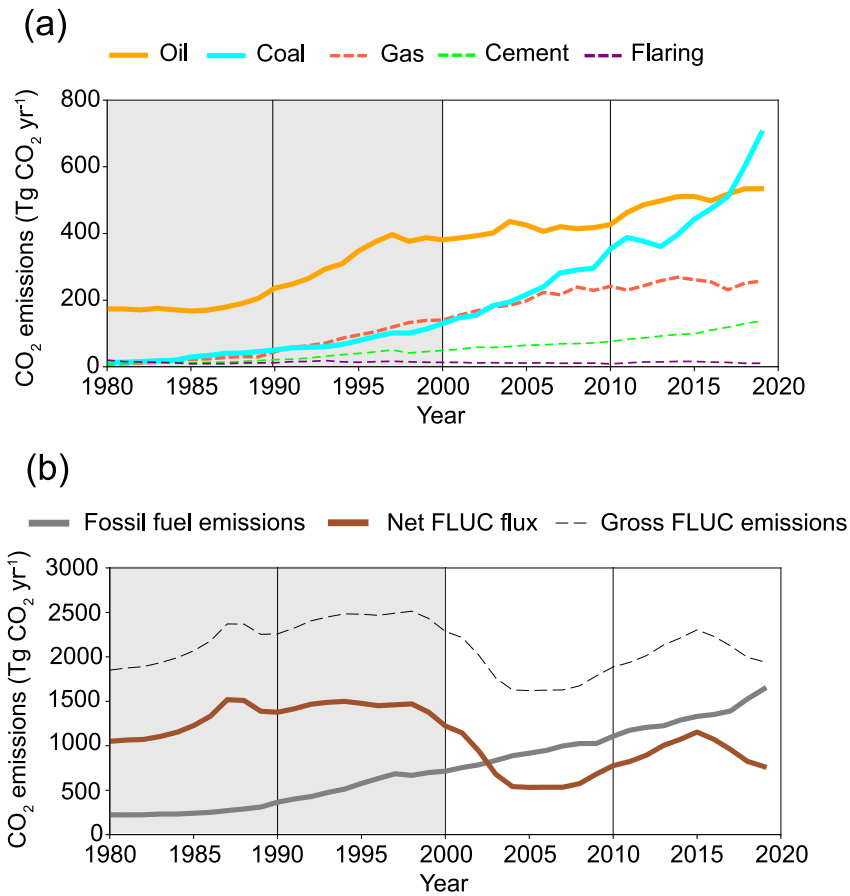


Figure 5. Interannual variation in anthropogenic carbon dioxide (CO_2) emissions contributed significantly to the GHG budget, from 1980 to 2019. (a) Interannual variability in CO_2 emissions from oil, gas, coal fuels, cement production, and gas flaring for 1980 to 2019. Two key emissions, CO_2 emissions from oil and coal fuels, are shown by bold lines, and the rest are represented by dashed lines. (b) Interannual variability in net LUC flux, gross LUC emissions (dashed line), and total fossil fuel CO_2 emissions (sum of CO_2 emissions from oil, gas, coal fuels, cement production, and gas flaring). The period prior to the target period for the GHG budget assessment is shown in gray shading.

anthropogenic CH_4 emissions, but the emissions from coal mining became dominant (42%) in the 2010s. Among N_2O emissions, waste-related N_2O emissions remained the largest component (65%) throughout the 2000s and the 2010s, displacing fossil fuel emissions. Nevertheless, these major CH_4 and N_2O emissions were substantially smaller than the CO_2 emissions from oil and coal fuels (less than 10%).

Among the nine major Southeast Asian countries, a large proportion of the top three GHG emissions from fossil fuels and waste (CO_2 emissions from oil, coal, and gas fuels) was found in Indonesia (~40%), followed by Thailand (~20%), Malaysia (~18%), Vietnam (~10%), and the Philippines (~8%) (Figures 4c and 4d). The order of these countries remained unchanged, although the top three emissions together increased by approximately 480 $TgCO_2\ yr^{-1}$. CO_2 emissions from oil fuels were the largest in all countries during the 2000s, except for Vietnam. This pattern remained the same during the 2010s, except that CO_2 emissions from coal fuel became the largest in Laos. Common to all countries, CO_2 emissions from coal fuels increased between the 2000s and the 2010s, with their decadal estimates in the 2010s becoming close to those from oil fuels.

4.3. Transitions of Anthropogenic GHG Emissions

The detailed investigation of anthropogenic GHG emissions highlights the evolving GHG emission landscape in Southeast Asia, revealing major emissions that characterize the net source of the current GHG budget in the region: CO_2 emissions from land-use changes in forests and from oil and coal fuels. Looking back from 1980 to 2019, CO_2 emissions from oil fuels dominated the rest from 1980 to 1999, with a continuously increasing pattern

19449224, 2025, 9, Downloaded from https://agupubs.onlinelibrary.wiley.com/doi/10.1029/2024GB008256 by Indian Institute Of Tech - Roorkee, Wiley Online Library on [14/03/2026]. See the Terms and Conditions (https://onlinelibrary.wiley.com/terms-and-conditions) on Wiley Online Library for rules of use; OA articles are governed by the applicable Creative Commons License

19449224, 2025, 9, Downloaded from https://agupubs.onlinelibrary.wiley.com/doi/10.1029/2024GB008256 by Indian Institute Of Tech - Roorkee, Wiley Online Library on [14/03/2026]. See the Terms and Conditions (https://onlinelibrary.wiley.com/terms-and-conditions) on Wiley Online Library for rules of use; OA articles are governed by the applicable Creative Commons License

(Figure 5a). However, even the total CO_2 emissions from fossil fuels, including oil, gas, and coal fuels, cement production, and gas flaring, were significantly lower than those from land-use changes in forests (gross FLUC emissions and net FLUC flux) during the same period, indicating that land-use changes in forests was by far the GHG emission source that most characterizes Southeast Asia in the past (Figure 5b).

Emissions from oil fuels increased from the 1980s through the late 1990s but remained relatively stable until the late 2000s, after which the rate of increase slowed until 2019 (Figure 5b). In contrast, CO_2 emissions from coal fuels have increased sharply since 2005 with an unprecedented rate of growth in the energy sector, surpassing CO_2 emissions from oil fuels in 2018 (Figure 5a). This suggests that coal fuels may become a major source of fossil fuel emissions in Southeast Asia in the near future. The shift from oil to coal use during 2000–2019 resulted in a continued increase in total CO_2 emissions from fossil fuels (Figure 5b).

The gross CO_2 emissions from land-use changes in forests, which were the largest source of GHG emissions in the region from 2000 to 2019, had even higher values for the long period from 1980 to 1999 (Figure 5b). It then declined significantly throughout the 2000s, and gradually increased from the late 2000s to the 2010s. In other words, focusing only on the period covered by this study, 2000–2019, it appears that land-use changes in forests simply became more active over the course of 20 years, but in fact, it was in a state of reactivity after recovering from the most active period in the 1990s.

These results suggest that a pivotal period for Southeast Asia was the 2000s, marked by stable CO_2 emissions from oil fuels (Figure 5a) and a significant reduction in gross FLUC emissions compared with the emissions released in the 1990s (Figure 5b). A previous study suggested that the decrease in gross FLUC emissions was due to economic factors, such as the Asian economic crisis of 1997–1998 and Indonesia's shift from wood production to plantations, which played a pivotal role in slowing down the loss of primary forests (Kondo et al., 2022). If Southeast Asian countries took advantage of this situation and initiated large-scale deforestation reduction and reforestation programs, the lower levels of CO_2 emissions in the 2000s (Figure 5b) could have persisted and even improved. Similarly, if Southeast Asian countries decided in the 2000s to shift their energy sources away from coal fuels and toward more efficient and cleaner natural gas and alternative energy resources, the increasing trend in CO_2 emissions could have been lowered.

However, CO_2 emissions from fossil fuels and land-use changes in forests showed a parallel increase during the 2010s (Figure 5b), which was enhanced by the rise in CO_2 emissions from coal fuels and the resumption of deforestation. Notably, although gross FLUC emissions were still dominant, the total CO_2 emissions from fossil fuels surpassed the net FLUC flux (inclusive of gross FLUC uptake) in the early 2000s, suggesting a transition from forestry to industry in Southeast Asia's economies. Recent findings based on the Global Energy Monitor (https://globalenergymonitor.org/projects/global-coal-plant-tracker/) revealed a concerning scenario. If all planned and under-constructed coal plants as of 2020 were to be operationalized, GHG emissions from the power sector in Southeast Asia could increase by 72% from 2020 to 2030 (Chen & Mauzerall, 2021). While it is unclear whether the increase in land-use changes in forests in the 2010s was temporary, it is necessary to monitor and sustain its associated CO_2 emissions so that they do not revert to those of the 1990s.

5. Uncertainty in GHG Budget Estimates

In this study, we strived to provide a comprehensive assessment of all major anthropogenic and natural sources and sinks of the three most important GHGs. We acknowledge that our budget estimates and fluxes comprising the GHG budget contained large uncertainties. One of the main issues with the GHG budget assessment for Southeast Asia is that local-scale dynamics may not be fully reflected in the estimates, owing to the lack of region-specific data. For example, in all peat-related GHG flux estimates, peatlands were treated and characterized as being static. However, the extent of peatlands in Southeast Asia has undergone dynamic changes owing to various anthropogenic influences over the past few decades. A recent study reported a peatland extent of approximately 13 Mha in Indonesia, indicating a reduction in its extent from the formerly reported area of 15–27 Mha (Anda et al., 2021). This large variability has significant implications for the quantification of GHG emissions released from fires and drained peatlands. Oil palm and rubber plantations are another set of key factors that characterize GHG emissions in Southeast Asia (Melton et al., 2022; Wang et al., 2023). However, they were classified together with other plantations for FLUC flux estimation (i.e., H&C), without reflecting the high productivity of these plantations in significantly shaping the estimates. The GHG fluxes of coastal ecosystems, particularly mangrove

19449224, 2025, 9, Downloaded from https://agupubs.onlinelibrary.wiley.com/doi/10.1029/2024GB008256 by Indian Institute Of Tech - Roorkee, Wiley Online Library on [14/03/2026]. See the Terms and Conditions (https://onlinelibrary.wiley.com/terms-and-conditions) on Wiley Online Library for rules of use; OA articles are governed by the applicable Creative Commons License

forests and seagrass meadows, are known to contain large carbon stocks per unit area (Bouillon et al., 2008); however, to date, their GHG fluxes have been poorly quantified.

The impact of fire emissions on GHG budgets may be lower than that indicated in this study. Extreme drought conditions associated with El Niño events have been identified as triggers for large and abrupt GHG emissions in Southeast Asia (Huijnen et al., 2016; Lohberger et al., 2017; Page et al., 2002; Siegert et al., 2001; Thirumalai et al., 2017; Vadrevu et al., 2019). Among the ENSO-sensitive fluxes, biomass burning, including peat burning is known to induce anomalous GHG emissions in the region (Page et al., 2002; Page & Hooijer, 2016). However, despite these well-known fire events in the region, independent atmospheric inverse model experiments, one using the column-average dry air-mole fraction of CO_2 from the Orbiting Carbon Observatory-2 (OCO-2) (Heymann et al., 2017) and the other utilizing CO_2 measurements from aircraft and ships over Southeast Asia (Niwa et al., 2021), reported that CO_2 emissions from fires in equatorial Southeast Asia during 2015 to be approximately 30% lower than those reported by GFEDv4s.

The natural vegetation flux (NEE), which was estimated through the TRENDY S2 simulation (no LULUCF effect), was the largest net sink component among all the GHG fluxes considered in this study; however, the range of the estimates was proportionally large (Table 1), implying that model sensitivity to atmospheric CO_2 and climate in the models is still a factor that confounds attempts to accurately estimate the GHG budget of Southeast Asia. Additionally, the natural vegetation flux represented by the TRENDY S2 simulation included the net CO_2 sink of undisturbed ecosystems, which should have been affected by LULUCF. Therefore, our estimate of the net CO_2 sink by natural vegetation may be partially overestimated by the uptake by non-existent natural ecosystems. Similarly, the wetland CH_4 emissions and natural soil N_2O fluxes, both based on process-based models, were the largest emission components of the CH_4 and N_2O budgets, with proportionally large uncertainties (Tables 2 and 3). Thus, reducing the estimation range of process-based models is the key to reducing the uncertainty of the GHG budget in the bottom-up approach. Although the contributions to the GHG budget were small, we need to address the wide range of estimates for global emission inventories, as evidenced by the estimates of CH_4 and N_2O emissions from agriculture and livestock (Tables 2 and 3).

In Southeast Asia, a region where atmospheric observations are scarce, the GHG fluxes estimated via atmospheric inversions inevitably have uncertainties embedded within them. In such situations, column-averaged CO_2 observations from satellites are expected to improve top-down GHG flux estimates. However, column-averaged GHG observations have their own issues regarding spatial biases, producing larger net sinks in northern temperate and boreal regions and larger net sources in tropical regions when assimilated into atmospheric inversions (Byrne et al., 2023; Houweling et al., 2015). In addition to the issue of data assimilation, an experiment conducted with MIROC4-ACTM revealed that the choice of prior land and ocean fluxes produced large regional sink/source variability (Chandra et al., 2022). The underlying reasons for the uncertainties in atmospheric inversions could be attributed to the fundamental model features, including the model resolution, control vector size, assimilation window length, transport model errors, and land-ocean separation (Kondo et al., 2020).

6. A Way Forward to Achieving Climate Neutrality

This study is the first to estimate the GHG budget for Southeast Asia, including all major anthropogenic and natural sources and sinks of CO_2, CH_4, and N_2O. We show that the region is a large net source of GHG, ranging from 3,226.3 ± 406.2 Tg CO_2eq yr^{-1} to 3,406.4 ± 572.9 Tg CO_2eq yr^{-1} for 2000–2019. We identified that the large net source of the GHG budget was largely driven by anthropogenic CO_2 emissions, such as land-use changes in forests and fossil fuels. Looking ahead to future energy policies within the context of the ASEAN region, the Long-range Energy Alternatives Planning model envisions a climate-neutral scenario, aiming to achieve climate neutrality (neutrality of all GHGs) by 2050 (Handayani et al., 2022). However, based on our estimates, the LEAPS model goal is not realistic, as it is unlikely that the increasing anthropogenic GHG emissions can be turned around quickly enough, and the remaining emissions will be offset over the next 25 years. Realistically, to meet the 1.5°C threshold target, in line with the scenarios proposed by the IPCC, effective plans should be implemented to achieve net-zero CO_2 emissions by 2050 and complete net-zero GHG emissions (including net-zero CH_4 and N_2O emissions) by 2070. Currently, some Southeast Asian countries are committed to achieving net-zero emissions by 2050 (e.g., Vietnam and Malaysia), and some of the largest emitters have set this target to 2060–65 (e.g., Indonesia and Thailand).

19449224, 2025, 9, Downloaded from https://agupubs.onlinelibrary.wiley.com/doi/10.1029/2024GB008256 by Indian Institute Of Tech - Roorkee, Wiley Online Library on [14/03/2026]. See the Terms and Conditions (https://onlinelibrary.wiley.com/terms-and-conditions) on Wiley Online Library for rules of use; OA articles are governed by the applicable Creative Commons License

The results of this study will help to effectively plan and set reduction targets that focus on sources with particularly high emissions rather than addressing all emission sources within a limited timeframe. CH_4 and N_2O emissions from agriculture and livestock sectors can be reduced by adopting precision agriculture, improving livestock management, and implementing sustainable agricultural practices. However, according to our assessment, GHG emissions from those sectors during 2000–2019 amounted to 466.0 Tg CO_{2eq} yr^{-1}, accounting for only 20% of the gross FLUC emissions. Instead, a more effective plan would focus on reducing CO_2 emissions from land-use changes in forests and fossil fuels, the most significant sources of GHG emissions in the region (totaling 3,058.5 Tg CO_2 yr^{-1} during 2000–2019), as reducing approximately 30% of these emissions offsets all anthropogenic CH_4 and N_2O emissions combined, including CH_4 and N_2O emissions from agriculture, livestock, peat drainage, and fires. Furthermore, limiting land-use changes in forests may promote ecosystem regeneration and lead to increased CO_2 uptake. Currently, land-use changes in Southeast Asia are a net source of GHGs, with emissions far exceeding the uptake by ecosystem regrowth and afforestation (Table 1). In northern temperate regions, the absence of land uses (abandonment of cropland) has resulted in hotspots of CO_2 uptake owing to the recovery of natural vegetation (Kondo, Ichii, Patra, Poulter, et al., 2018; Pugh et al., 2019). It may be possible to induce hotspots of CO_2 uptake in Southeast Asia by promoting afforestation, in addition to limiting land-use changes such as wood harvesting and shifting cultivation, thereby restoring the region's naturally productive forests. GHG emissions from fires should also be included as reduction targets for Southeast Asia. This is not only because fires are the second largest source of CO_2 emissions after land-use changes in forests, but also they remain a major environmental and social issue in Southeast Asian countries, leading to high concentrations of pollutants being released into the atmosphere (causing hazardous haze), posing a threat to human health, aviation, and the environmental well-being of the region (Crippa et al., 2016; Othman et al., 2022; Tan-Soo & Pattanayak, 2018).

To make these reduction targets a reality, it is essential to address uncertainties and refine GHG budget estimates in Southeast Asia so that they can be downscaled to a national scale. Southeast Asian countries are diverse in terms of climate, vegetation distribution, and economic development; therefore, their GHG budgets and mitigation opportunities vary significantly. As this study shows, Indonesia, which is responsible for much of the CO_2 emissions from land-use changes in forests and fossil fuels (Figures 3c, 3d, 4c, and 4d), must play a central role in achieving climate neutrality in Southeast Asia as a whole. However, we note that mitigation and net-zero emission targets under the Paris Agreement are nationally determined, and therefore, the responsibility for achieving them lies with individual nation-states. In contrast to developed countries, where fossil fuels account for the majority of GHG emissions, Southeast Asia is undergoing rapid economic development, making it particularly challenging to pursue a pathway that achieves climate neutrality and sustained economic growth.

Even with the latest data set prepared by RECCAP2, some of the data are statistical estimates that only cover the entire region of Southeast Asia and cannot be downscaled into detailed values on a national scale. To overcome these challenges, we launched an international network to facilitate the quantification of GHG fluxes in Southeast Asia, namely, the League of geophysical research eXcellences for tropical Asia (LeXtra). LeXtra continues to improve GHG fluxes and monitoring in Southeast Asia's GHG budget, while enabling the identification of the detailed contributions from each country in Southeast Asia, which could not be addressed in this study. This effort will be supported and be a contribution to the Global Carbon Project's new REgional Carbon Cycle Assessment and Processes, Phase 3 (RECCAP3), which will particularly focus on national-level GHG budgets (Canadell et al., 2025).

Conflict of Interest

The authors declare no conflicts of interest relevant to this study.

Data Availability Statement

All data used in this study are publicly available from the data repository of RECCAP-2 (https://www.bgc-jena.mpg.de/geodb/projects/Home.php), the Global Carbon Budget 2022 (Friedlingstein et al., 2022), IEA2023 (https://www.iea.org/), EDGARv7.0 (https://edgar.jrc.ec.europa.eu/dataset_ghg70), CEDSv2021 (https://zenodo.org/records/4741285), FAOSTAT (http://www.fao.org/faostat/en/#data), and individual sources. Weathering CO_2 uptake, book-keeping estimates of gross FLUC emissions and uptake, river carbon exports, coastal

19449224, 2025, 9, Downloaded from https://agupubs.onlinelibrary.wiley.com/doi/10.1029/2024GB008256 by Indian Institute Of Tech - Roorkee, Wiley Online Library on [14/03/2026]. See the Terms and Conditions (https://onlinelibrary.wiley.com/terms-and-conditions) on Wiley Online Library for rules of use; OA articles are governed by the applicable Creative Commons License

vegetation fluxes, wood and crop trade, wetland CH_4 emissions, N_2O fluxes of natural soils, and a majority of CO_2, CH_4, and N_2O inversions are available from the data repository of RECCAP-2. CO_2 and CH_4 emissions from oil, coal, and gas are available from IEA2023, and N_2O emissions from oil, coal, and gas, are available from EDGARv7.0. CO_2 emissions from Cement production and gas flaring are available from the Global Carbon Budget 2022. CH_4 and N_2O emissions from waste disposal and burning are available from EDGARv7.0 and CEDSv2021. GHG emissions from manure management, enteric fermentation, rice cultivation, and agricultural soils are available from FAOSTAT, EDGARv7.0, and CEDSv2021. GHG emissions from fire are available from FAOSTAT and GFEDs4.1 (https://www.globalfiredata.org/data.html). Geological seepage data are available from Etiope et al. (2019) (https://gml.noaa.gov/ccgg/arc/index.php?id=130). CO_2, CH_4 and N_2O outgassing from lakes and rivers are available from Lauerwald et al. (2023) (https://doi.org/10.6084/m9.figshare.22492504). TRENDY data are available via Profs. Stephen Sitch and Pierre Friedlingstein, Exeter University (s.a.sitch@exeter.ac.uk; p.friedlingstein@exeter.ac.uk). VISIT simulations for oxidative CH_4 consumption and termite CH_4 emissions are available via Prof. Akihiko Ito, the Tokyo University (akihikoito@g.ecc.u-tokyo.ac.jp). Three CO_2 inversions, ACTM_CONTRAIL, JMA2021, and GOSAT L4A are available via Dr. Tazu Saeki (saeki.tazu@nies.go.jp), Dr. Takashi Maki (tmaki@mri-jma.go.jp), and from the GOSAT data portal (https://data2.gosat.nies.go.jp/index_en.html), respectively. All data sets used in this study were listed in Tables S1–S6 in Supporting Information S1 with detailed data descriptions and link for access.

Acknowledgments

This paper is a contribution to the REgional Carbon Cycle Assessment and Processes (RECCAP) Phase 2 coordinated by the Global Carbon Project, and to the League of geophysical research eXcellences for tropical Asia (LeXtra) sponsored by Integrated Land Ecosystem-Atmosphere Processes Study (iLEAPS). P.K.P. and N.C. were supported by the Arctic Challenge for Sustainability II (ArCS-II) project (Grant JPMXD1420318865), funded by Japan's Ministry of Education, Culture, Sports, Science and Technology (MEXT). A.I. was supported by the Environmental and Technology Development Fund (JPMEERF21S20800) of the Environmental Restoration and Conservation Agency of Japan. T.M. was supported by the JSPS KAKENHI (Grant numbers: JP19K12312), Environment Research and Technology Development Fund (JPMEERF21S20810) of the Environmental Restoration and Conservation Agency of Japan from the Ministry of the Environment, Japan. R.L. acknowledges funding from French state aid, managed by ANR under the "Investissements d'avenir" programme (ANR-16-CONV-0003). A. K. J. was supported by NASA LCLUC program (grant number: 80NSSC24K0920). We express our deep gratitude to all the researchers who were involved in this research and RECCAP2 through project management, data provision, and discussions.

References

Achard, F., Beuchle, R., Mayaux, P., Stibig, H.-J., Bodart, C., Brink, A., et al. (2014). Determination of tropical deforestation rates and related carbon losses from 1990 to 2010. *Global Change Biology*, *20*(8), 2540–2554. https://doi.org/10.1111/gcb.12605

Allen, G. H., & Pavelsky, T. M. (2018). Global extent of rivers and streams. *Science*, *361*(6402), 585–588. https://doi.org/10.1126/science.aat0636

Anda, M., Ritung, S., Suryani, E., Hikmat, M., Yatno, E., Mulyani, A., et al. (2021). Revisiting tropical peatlands in Indonesia: Semi-detailed mapping, extent and depth distribution assessment. *Geoderma*, *402*, 115235. https://doi.org/10.1016/j.geoderma.2021.115235

Andrew, R. M. (2018). Global CO_2 emissions from cement production. *Earth System Science Data*, *10*(1), 195–217. https://doi.org/10.5194/essd-10-195-2018

Baccini, A., Walker, W., Carvalho, L., Farina, M., Sulla-Menashe, D., & Houghton, R. A. (2017). Tropical forests are a net carbon source based on aboveground measurements of gain and loss. *Science*, *358*(6360), 230–234. https://doi.org/10.1126/science.aam5962

Bergamaschi, P., Houweling, S., Segers, A., Krol, M., Frankenberg, C., Scheepmaker, R. A., et al. (2013). Atmospheric CH_4 in the first decade of the 21st century: Inverse modeling analysis using SCIAMACHY satellite retrievals and NOAA surface measurements. *Journal of Geophysical Research-Atmospheres*, *118*(13), 7350–7369. https://doi.org/10.1002/jgrd.50480

Bouillon, S., Borges, A. V., Castañeda-Moya, E., Diele, K., Dittmar, T., Duke, N. C., et al. (2008). Mangrove production and carbon sinks: A revision of global budget estimates. *Global Biogeochemical Cycles*, *22*, GB2013. https://doi.org/10.1029/2007GB003052

Byrne, B., Baker, D. F., Basu, S., Bertolacci, M., Bowman, K. W., Carroll, D., et al. (2023). National CO_2 budgets (2015–2020) inferred from atmospheric CO_2 observations in support of the global stocktake. *Earth System Science Data*, *15*(2), 963–1004. https://doi.org/10.5194/essd-15-963-2023

Cai, W., Wu, L., Lengaigne, M., Li, T., McGregor, S., Kug, J.-S., et al. (2019). Pantropical climate interactions. *Science*, *363*, 6430. https://doi.org/10.1126/science.aav4236

Canadell, J. G., Monteiro, P. M., Costa, M. H., Da Cunha, L. C., Cox, P. M., Alexey, V., et al. (2021). Global carbon and other biogeochemical cycles and feedbacks. In V. Masson-Delmotte, P. Zhai, A. Pirani, S. L. Connors, C. Péan, S. Berger, et al. (Eds.), *Climate change 2021: The physical science basis. Contribution of working group I to the sixth assessment report of the intergovernmental Panel on climate change* (pp. 673–816). Cambridge University Press. https://doi.org/10.1017/9781009157896.007

Canadell, J. G., Poulter, B., Bastos, A., Ciais, P., Hauck, J., Andrew, R., et al. (2025). From global to national GHG budgets: The Regional carbon cycle assessment and processes-3 (RECCAP3). *National Science Review*, *12*(4), nwaf037. https://doi.org/10.1093/nsr/nwaf037

Carlson, K. M., Curran, L. M., Ratnasari, D., Pittman, A. M., Soares-Filho, B. S., Asner, G. P., et al. (2012). Committed carbon emissions, deforestation, and community land conversion from oil palm plantation expansion in West Kalimantan, Indonesia. *Proceedings of the National Academy of Sciences of the United States of America*, *109*(19), 7559–7564. https://doi.org/10.1073/pnas.1200452109

Carlson, K. M., Heilmayr, R., Gibbs, H. K., Noojipady, P., Burns, D. N., Morton, D. C., et al. (2018). Effect of oil palm sustainability certification on deforestation and fire in Indonesia. *Proceedings of the National Academy of Sciences of the United States of America*, *115*(1), 121–126. https://doi.org/10.1073/pnas.1704728114

Chandra, N., Patra, P. K., Bisht, J. S. H., Ito, A., Umezawa, T., Saigusa, N., et al. (2021). Emissions from the oil and gas sectors, coal mining and ruminant farming drive methane growth over the past three decades. *Journal of the Meteorological Society of Japan. Ser. II*, *99*(2), 309–337. https://doi.org/10.2151/jmsj.2021-015

Chandra, N., Patra, P. K., Niwa, Y., Ito, A., Iida, Y., Goto, D., et al. (2022). Estimated regional CO_2 flux and uncertainty based on an ensemble of atmospheric CO_2 inversions. *Atmospheric Chemistry and Physics*, *22*(14), 9215–9243. https://doi.org/10.5194/acp-22-9215-2022

Chen, X., & Mauzerall, D. L. (2021). The expanding coal power fleet in Southeast Asia: Implications for future CO_2 emissions and electricity generation. *Earth's Future*, *9*(12), e2021EF002257. https://doi.org/10.1029/2021EF002257

Chevallier, F., Ciais, P., Conway, T. J., Aalto, T., Anderson, B. E., Bousquet, P., et al. (2010). CO_2 surface fluxes at grid point scale estimated from a global 21 year reanalysis of atmospheric measurements. *Journal of Geophysical Research*, *115*(D21), D21307. https://doi.org/10.1029/2010JD013887

Chini, L., Hurtt, G., Sahajpal, R., Frolking, S., Klein Goldewijk, K., Sitch, S., et al. (2021). Land-use harmonization datasets for annual global carbon budgets. *Earth System Science Data*, *13*(8), 4175–4189. https://doi.org/10.5194/essd-13-4175-2021

Ciais, P., Bastos, A., Chevallier, F., Lauerwald, R., Poulter, B., Canadell, J. G., et al. (2022). Definitions and methods to estimate regional land carbon fluxes for the second phase of the REgional Carbon Cycle Assessment and Processes Project (RECCAP-2). *Geoscientific Model Development*, *15*(3), 1289–1316. https://doi.org/10.5194/gmd-15-1289-2022

Crippa, M., Guizzardi, D., Pagani, F., Banja, M., Muntean, M., Schaaf, E., et al. (2023). *GHG emissions of all world countries*. Publications Office of the European Union. JRC134504. https://doi.org/10.2760/953322

Crippa, P., Castruccio, S., Archer-Nicholls, S., Lebron, G. B., Kuwata, M., Thota, A., et al. (2016). Population exposure to hazardous air quality due to the 2015 fires in Equatorial Asia. *Scientific Reports*, *6*(1), 37074. https://doi.org/10.1038/srep37074

Curry, C. L. (2007). Modeling the soil consumption of atmospheric methane at the global scale. *Global Biogeochemical Cycles*, *21*(4), GB4012. https://doi.org/10.1029/2006GB002818

Etiope, G., Ciotoli, G., Schwietzke, S., & Schoell, M. (2019). Gridded maps of geological methane emissions and their isotopic signature. *Earth System Science Data*, *11*, 1–22. https://doi.org/10.5194/essd-11-1-2019

Feng, L., Palmer, P. I., Parker, R. J., Deutscher, N. M., Feist, D. G., Kivi, R., et al. (2016). Estimates of European uptake of CO_2 inferred from GOSAT XCO_2 retrievals: Sensitivity to measurement bias inside and outside Europe. *Atmospheric Chemistry and Physics*, *16*(3), 1289–1302. https://doi.org/10.5194/acp-16-1289-2016

Field, R. D., van der Werf, G. R., & Shen, S. S. P. (2009). Human amplification of drought-induced biomass burning in Indonesia since 1960. *Nature Geoscience*, *2*(3), 185–188. https://doi.org/10.1038/ngeo443

Food and Agriculture Organization (FAO). (2020). Global forest resources assessment 2020: Main report, Rome, Italy.

Forster, P., Storelvmo, T., Armour, K., Collins, W., Dufresne, J.-L., Frame, D., et al. (2021). The Earth's energy budget, climate feedbacks, and climate sensitivity. In V. Masson-Delmotte, P. Zhai, A. Pirani, S. L. Connors, C. Péan, S. Berger, et al. (Eds.), *Climate change 2021: The physical science basis. Contribution of working group I to the sixth assessment report of the intergovernmental Panel on climate change* (pp. 923–1054). Cambridge University Press. https://doi.org/10.1017/9781009157896.009

Friedlingstein, P., Jones, M. W., O'Sullivan, M., Andrew, R. M., Bakker, D. C. E., Hauck, J., et al. (2022). Global carbon budget 2021. *Earth System Science Data*, *14*(4), 1917–2005. https://doi.org/10.5194/essd-14-1917-2022

Giglio, L., Boschetti, L., Roy, D. P., Humber, M. L., & Justice, C. O. (2018). The Collection 6 MODIS burned area mapping algorithm and product. *Remote Sensing of Environment*, *217*, 72–85. https://doi.org/10.1016/j.rse.2018.08.005

Handayani, K., Anugrah, P., Goembira, F., Overland, I., Suryadi, B., & Swandaru, A. (2022). Moving beyond the NDCs: ASEAN pathways to a net-zero emissions power sector in 2050. *Applied Energy*, *311*, 118580. https://doi.org/10.1016/j.apenergy.2022.118580

Hansis, E., Davis, S. J., & Pongratz, J. (2015). Relevance of methodological choices for accounting of land use change carbon fluxes. *Global Biogeochemical Cycles*, *29*(8), 1230–1246. https://doi.org/10.1002/2014gb004997

Hartmann, J., Jansen, N., Dürr, H. H., Kempe, S., & Köhler, P. (2009). Global CO_2-consumption by chemical weathering: What is the contribution of highly active weathering regions? *Global and Planetary Change*, *69*(4), 185–194. https://doi.org/10.1016/j.gloplacha.2009.07.007

Heymann, J., Reuter, M., Buchwitz, M., Schneising, O., Bovensmann, H., Burrows, J. P., et al. (2017). CO_2 emission of Indonesian fires in 2015 estimated from satellite-derived atmospheric CO_2 concentrations. *Geophysical Research Letters*, *44*(3), 1537–1544. https://doi.org/10.1002/2016GL072042

Hooijer, A., Page, S., Canadell, J. G., Silvius, M., Kwadijk, J., Wösten, H., & Jauhiainen, J. (2010). Current and future CO_2 emissions from drained peatlands in Southeast Asia. *Biogeosciences*, *7*(5), 1505–1514. https://doi.org/10.5194/bg-7-1505-2010

Hooijer, A., Page, S., Jauhiainen, J., Lee, W. A., Lu, X. X., Idris, A., & Anshari, G. (2012). Subsidence and carbon loss in drained tropical peatlands. *Biogeosciences*, *9*(3), 1053–1071. https://doi.org/10.5194/bg-9-1053-2012

Houghton, R. A., & Castanho, A. (2023). Annual emissions of carbon from land use, land-use change, and forestry from 1850 to 2020. *Earth System Science Data*, *15*(5), 2025–2054. https://doi.org/10.5194/essd-15-2025-2023

Houghton, R. A., & Nassikas, A. A. (2017). Global and regional fluxes of carbon from land use and land cover change 1850–2015. *Global Biogeochemical Cycles*, *31*(3), 456–472. https://doi.org/10.1002/2016GB005546

Houweling, S., Baker, D., Basu, S., Boesch, H., Butz, A., Chevallier, F., et al. (2015). An intercomparison of inverse models for estimating sources and sinks of CO_2 using GOSAT measurements. *Journal of Geophysical Research-Atmosphere*, *120*(10), 5253–5266. https://doi.org/10.1002/2014JD022962

Huijnen, V., Wooster, M. J., Kaiser, J. W., Gaveau, D. L. A., Flemming, J., Parrington, M., et al. (2016). Fire carbon emissions over maritime southeast Asia in 2015 largest since 1997. *Scientific Reports*, *6*(1), 26886. https://doi.org/10.1038/srep26886

IPCC. (2006). In H. S. Eggleston, L. Buendia, K. Miwa, T. Ngara, & K. Tanabe (Eds.), *2006 IPCC guidelines for national greenhouse gas inventories, prepared by the national greenhouse gas inventories programme*. IGES.

IPCC. (2014). In T. Hiraishi, T. Krug, K. Tanabe, N. Srivastava, J. Baasansuren, M. Fukuda, & T. G. Troxler. (Eds.), *2013 supplement to the 2006 IPCC guidelines for national greenhouse gas inventories: Wetlands*. IPCC. Switzerland.

Ishizawa, M., Mabuchi, K., Shirai, T., Inoue, M., Morino, I., Uchino, O., et al. (2016). Interannual variability of summertime CO_2 exchange in Northern Eurasia inferred from GOSAT XCO_2. *Environmental Research Letters*, *11*(10), 105001. https://doi.org/10.1088/1748-9326/11/10/105001

Ito, A. (2023). Global termite methane emissions have been affected by climate and land-use changes. *Scientific Reports*, *13*(1), 17195. https://doi.org/10.1038/s41598-023-44529-1

Ito, A., Patra, P. K., & Umezawa, T. (2023). Bottom-up evaluation of the methane budget in Asia and its subregions. *Global Biogeochemical Cycles*, *37*(6), e2023GB007723. https://doi.org/10.1029/2023GB007723

Kondo, M., Ichii, K., Patra, P. K., Canadell, J. G., Poulter, B., Sitch, S., et al. (2018). Land use change and El Niño-Southern Oscillation drive decadal carbon balance shifts in Southeast Asia. *Nature Communications*, *9*(1), 1154. https://doi.org/10.1038/s41467-018-03374-x

Kondo, M., Ichii, K., Patra, P. K., Poulter, B., Calle, L., Koven, C., et al. (2018). Plant regrowth as a driver of recent enhancement of terrestrial CO_2 uptake. *Geophysical Research Letters*, *45*(10), 4820–4830. https://doi.org/10.1029/2018GL077633

Kondo, M., Patra, P. K., Sitch, S., Friedlingstein, P., Poulter, B., Chevallier, F., et al. (2020). State of the science in reconciling top-down and bottom-up approaches for terrestrial CO_2 budget. *Global Change Biology*, *20*(3), 1068–1084. https://doi.org/10.1111/gcb.14917

Kondo, M., Sitch, S., Ciais, P., Achard, F., Kato, E., Pongratz, J., et al. (2022). Are land-use change emissions in Southeast Asia decreasing or increasing? *Global Biogeochemical Cycles*, *36*(1), e2020GB006909. https://doi.org/10.1029/2020GB006909

Lauerwald, R., Allen, G., Deemer, B., Liu, S., Maavara, T., Raymond, P., et al. (2023). Inland water greenhouse gas budgets for RECCAP2: 2 regionalization and homogenization of estimates following the RECCAP2 framework. *Global Biogeochemical Cycles*, *37*(5), e2022GB007658. https://doi.org/10.1029/2022GB007658

Li, W., MacBean, N., Ciais, P., Defourny, P., Lamarche, C., Bontemps, S., et al. (2018). Gross and net land cover changes in the main plant functional types derived from the annual ESA CCI land cover maps (1992–2015). *Earth System Science Data*, *10*(1), 219–234. https://doi.org/10.5194/essd-10-219-2018

Liu, J., Baskaran, L., Bowman, K., Schimel, D., Bloom, A. A., Parazoo, N. C., et al. (2021). Carbon monitoring system flux net biosphere exchange 2020 (CMS-Flux NBE 2020). *Earth System Science Data*, *13*(2), 299–330. https://doi.org/10.5194/essd-13-299-2021

19449224, 2025, 9, Downloaded from https://agupubs.onlinelibrary.wiley.com/doi/10.1029/2024GB008256 by Indian Institute Of Tech - Roorkee, Wiley Online Library on [14/03/2026]. See the Terms and Conditions (https://onlinelibrary.wiley.com/terms-and-conditions) on Wiley Online Library for rules of use; OA articles are governed by the applicable Creative Commons License

Lohberger, S., Stängel, M., Atwood, E. C., & Siegert, F. (2017). Spatial evaluation of Indonesia's 2015 fire-affected area and estimated carbon emissions using Sentinel-1. *Global Change Biology*, *24*(2), 644–654. https://doi.org/10.1111/gcb.13841

Machida, T., Matsueda, H., Sawa, Y., Nakagawa, Y., Hirotani, K., Kondo, N., et al. (2008). Worldwide measurements of atmospheric CO_2 and other trace gas species using commercial airlines. *Journal of Atmospheric and Oceanic Technology*, *25*(10), 1744–1754. https://doi.org/10.1175/2008JTECHA1082.1

Maki, T., Kondo, K., Ishijima, Sekiyama, T. T., Tsuboi, K., & Nakamura, T. (2023). Independent bias correction method for satellite observation data introduced to CO_2 flux inversion. *SOLA*, *19*, 157–164. https://doi.org/10.2151/sola.2023-021

Maksyutov, S., Oda, T., Saito, M., Janardanan, R., Belikov, D., Kaiser, J. W., et al. (2021). Technical note: A high-resolution inverse modelling technique for estimating surface CO_2 fluxes based on the NIES-TM–FLEXPART coupled transport model and its adjoint. *Atmospheric Chemistry and Physics*, *21*(2), 1245–1266. https://doi.org/10.5194/acp-21-1245-2021

Maksyutov, S., Takagi, H., Valsala, V. K., Saito, M., Oda, T., Saeki, T., et al. (2013). Regional CO_2 flux estimates for 2009–2010 based on GOSAT and ground-based CO_2 observations. *Atmospheric Chemistry and Physics*, *13*(18), 9351–9373. https://doi.org/10.5194/acp-13-9351-2013

Matsueda, H., Machida, T., Sawa, Y., Nakagawa, Y., Hirotani, K., Ikeda, H., et al. (2008). Evaluation of atmospheric CO_2 measurements from new flask air sampling of JAL airliner observations. *Papers in Meteorology and Geophysics*, *59*, 1–17. https://doi.org/10.2467/mripapers.59.1

Mayorga, E., Seitzinger, S. P., Harrison, J. A., Dumont, E., Beusen, A. H. W., Bouwman, A. F., et al. (2010). Global nutrient export from WaterSheds 2 (NEWS 2): Model development and implementation. *Environmental Modelling & Software*, *25*(7), 837–853. https://doi.org/10.1016/j.envsoft.2010.01.007

McDuffie, E. E., Smith, S. J., O'Rourke, P., Tibrewal, K., Venkataraman, C., Marais, E. A., et al. (2020). A global anthropogenic emission inventory of atmospheric pollutants from sector- and fuel-specific sources (1970–2017): An application of the community emissions data system (CEDS). *Earth System Science Data*, *12*(4), 3413–3442. https://doi.org/10.5194/essd-12-3413-2020

McNorton, J., Wilson, C., Gloor, M., Parker, R. J., Boesch, H., Feng, W., et al. (2018). Attribution of recent increases in atmospheric methane through 3-D inverse modelling. *Atmospheric Chemistry and Physics*, *18*(24), 18149–18168. https://doi.org/10.5194/acp-18-18149-2018

Melton, J. R., Chan, E., Millard, K., Fortier, M., Winton, R. S., Martín-López, J. M., et al. (2022). A map of global peatland extent created using machine learning (Peat-ML). *Geoscientific Model Development*, *15*(12), 4709–4738. https://doi.org/10.5194/gmd-15-4709-2022

Messager, M. L., Lehner, B., Grill, G., Nedeva, I., & Schmitt, O. (2016). Estimating the volume and age of water stored in global lakes using a geostatistical approach. *Nature Communications*, *7*(1), 13603. https://doi.org/10.1038/ncomms13603

Miettinen, J., Shi, C., & Liew, S. C. (2016). Land-cover distribution in the peatlands of peninsular Malaysia, Sumatra and borneo in 2015 with changes since 1990. *Global Ecology and Conservation*, *6*, 67–78. https://doi.org/10.1016/j.gecco.2016.02.004

Mitchard, E. T. A. (2018). The tropical forest carbon cycle and climate change. *Nature*, *559*(7715), 527–534. https://doi.org/10.1038/s41586-018-0300-2

Murdiyarso, D., Hergoualc'h, K., & Verchot, L. V. (2010). Opportunities for reducing greenhouse gas emissions in tropical peatlands. *Proceedings of the National Academy of Sciences of the United States of America*, *107*(46), 19655–19660. https://doi.org/10.1073/pnas.0911966107

Myers, N., Mittermeier, R. A., Mittermeier, C. G., da Fonseca, G. A. B., & Kent, J. (2000). Biodiversity hotspots for conservation priorities. *Nature*, *403*(6772), 853–858. https://doi.org/10.1038/35002501

Niwa, Y., Fujii, Y., Sawa, Y., Iida, Y., Ito, A., Satoh, M., et al. (2017). A 4D-Var inversion system based on the icosahedral grid model (NICAM-TM 4DVar v1.0) – Part 2: Optimization scheme and identical twin experiment of atmospheric CO_2 inversion. *Geoscientific Model Development*, *10*(6), 2201–2219. https://doi.org/10.5194/gmd-10-2201-2017

Niwa, Y., Sawa, Y., Nara, H., Machida, T., Matsueda, H., Umezawa, T., et al. (2021). Estimation of fire-induced carbon emissions from Equatorial Asia in 2015 using in situ aircraft and ship observations. *Atmospheric Chemistry and Physics*, *21*(12), 9455–9473. https://doi.org/10.5194/acp-21-9455-2021

Niwa, Y., Tomita, H., Satoh, M., Imasu, R., Sawa, Y., Tsuboi, K., et al. (2017). A 4D-Var inversion system based on the icosahedral grid model (NICAM-TM 4D-Var v1.0) – Part 1: Offline forward and adjoint transport models. *Geoscientific Model Development*, *10*(3), 1157–1174. https://doi.org/10.5194/gmd-10-1157-2017

Othman, M., Latif, M. T., Hamid, H. H. A., Uning, R., Khumsaeng, T., Phairuang, W., et al. (2022). Spatial–temporal variability and health impact of particulate matter during a 2019–2020 biomass burning event in Southeast Asia. *Scientific Reports*, *12*(1), 7630. https://doi.org/10.1038/s41598-022-11409-z

Page, S. E., & Hooijer, A. (2016). In the line of fire: The peatlands of Southeast Asia. *Philosophical Transactions of the Royal Society B*, *371*(1696), 20150176. https://doi.org/10.1098/rstb.2015.0176

Page, S. E., Siegert, F., Rieley, J. O., Boehm, H.-D. V., Jaya, A., & Limin, S. (2002). The amount of carbon released from peat and forest fires in Indonesia during 1997. *Nature*, *420*(6911), 61–65. https://doi.org/10.1038/nature01131

Pandey, S., Houweling, S., Krol, M., Aben, I., Chevallier, F., Dlugokencky, E. J., et al. (2016). Inverse modeling of GOSAT-retrieved ratios of total column CH_4 and CO_2 for 2009 and 2010. *Atmospheric Chemistry and Physics*, *16*(8), 5043–5062. https://doi.org/10.5194/acp-16-5043-2016

Patra, P. K., Saeki, T., Dlugokencky, E. J., Ishijima, K., Umezawa, T., Ito, A., et al. (2016). Regional methane emission estimation based on observed atmospheric concentrations (2002–2012). *Journal of the Meteorological Society of Japan*, *94*(1), 85–107. https://doi.org/10.2151/jmsj.2016-006

Patra, P. K., Takigawa, M., Watanabe, S., Chandra, N., Ishijima, K., & Yamashita, Y. (2018). Improved chemical tracer simulation by MIROC4.0-based atmospheric chemistry-transport model (MIROC4-ACTM). *SOLA*, *14*, 91–96. https://doi.org/10.2151/sola.2018-016

Peters, W., Jacobson, A. R., Sweeney, C., Andrews, A. E., Conway, T. J., Masarie, K., et al. (2007). An atmospheric perspective on North American carbon dioxide exchange: Carbon tracker. *Proceedings of the National Academy of Sciences*, *104*(48), 18925–18930. https://doi.org/10.1073/pnas.0708986104

Poulter, B., Bastos, A., Canadell, J. G., Ciais, P., Gruber, N., Hauck, J., et al. (2022). Inventorying Earth's land and ocean greenhouse gases. *Eos*, *103*. https://doi.org/10.1029/2022EO179084

Pugh, T. A. M., Lindeskog, M., Smith, B., Poulter, B., Arneth, A., Haverd, V., & Calle, L. (2019). Role of forest regrowth in global carbon sink dynamics. *Proceedings of the National Academy of Sciences of the United States of America*, *116*(10), 4382–4387. https://doi.org/10.1073/pnas.1810512116

Qiu, J., Seah, S., & Martinus, M. (2024). Examining climate ambition enhancement in ASEAN countries' nationally determined contributions. *Environmental Development*, *49*, 100945. https://doi.org/10.1016/j.envdev.2023.100945

Raymond, P. A., Hartmann, J., Lauerwald, R., Sobek, S., McDonald, C., Hoover, M., et al. (2013). Global carbon dioxide emissions from inland waters. *Nature*, *503*, 355–359. https://doi.org/10.1038/nature13142

19449224, 2025, 9, Downloaded from https://agupubs.onlinelibrary.wiley.com/doi/10.1029/2024GB008256 by Indian Institute Of Tech - Roorkee, Wiley Online Library on [14/03/2026]. See the Terms and Conditions (https://onlinelibrary.wiley.com/terms-and-conditions) on Wiley Online Library for rules of use; OA articles are governed by the applicable Creative Commons License

Richards, D. R., & Friess, D. A. (2015). Rates and drivers of mangrove deforestation in Southeast Asia, 2000–2012. *Proceedings of the National Academy of Sciences of the United States of America*, *113*(2), 344–349. https://doi.org/10.1073/pnas.1510272113

Rosentreter, J. A., Laruelle, G. G., Bange, H. W., Bianchi, T. S., Busecke, J. J. M., Cai, W.-J., et al. (2023). Coastal vegetation and estuaries are collectively a greenhouse gas sink. *Nature Climate Change*, *13*(6), 579–587. https://doi.org/10.1038/s41558-023-01682-9

Saeki, T., & Patra, P. K. (2017). Implications of overestimated anthropogenic CO_2 emissions on East Asian and global land CO_2 flux inversion. *Geoscience Letters*, *4*(1), 9. https://doi.org/10.1186/s40562-017-0074-7

Saunois, M., Stavert, A. R., Poulter, B., Bousquet, P., Canadell, J. G., Jackson, R. B., et al. (2020). The global methane budget 2000–2017. *Earth System Science Data*, *12*(3), 1561–1623. https://doi.org/10.5194/essd-12-1561-2020

Segers, A., & Houweling, S. (2018). Description of the CH_4 inversion production chain, CAMS (copernicus atmospheric monitoring service) report. Retrieved from https://atmosphere.copernicus.eu/sites/default/files/2018-11/CAMS73_2015SC3_D73.2.5.5-2018_201811_production_chain_v1_0.pdf

Siegert, F., Ruecker, G., Hinrichs, A., & Hoffmann, A. A. (2001). Increased damage from fires in logged forests during droughts caused by El Nino. *Nature*, *414*(6862), 437–440. https://doi.org/10.1038/35106547

Sodhi, N. S., Koh, L. P., Brook, B. W., & Ng, P. K. L. (2004). Southeast Asian biodiversity: An impending disaster. *Trends in Ecology and Evolution*, *12*(19), 654–660. https://doi.org/10.1016/j.tree.2004.09.006

Sodhi, N. S., Posa, M. R. C., Lee, T. M., Bickford, D., Koh, L. P., & Brook, B. W. (2010). The state and conservation of Southeast Asian biodiversity. *Biodiversity & Conservation*, *19*(2), 317–328. https://doi.org/10.1007/s10531-009-9607-5

Stibig, H.-J., Achard, F., Carboni, S., Raši, R., & Miettinen, J. (2014). Change in tropical forest cover of Southeast Asia from 1990 to 2010. *Biogeosciences*, *11*(2), 247–258. https://doi.org/10.5194/bg-11-247-2014

Tan-Soo, J.-S., & Pattanayak, S. K. (2018). Seeking natural capital projects: Forest fires, haze, and early-life exposure in Indonesia. *Proceedings of the National Academy of Sciences of the United States of America*, *116*(12), 5239–5245. https://doi.org/10.1073/pnas.1802876116

Thirumalai, K., DiNezio, P. N., Okumura, Y., & Deser, C. (2017). Extreme temperatures in Southeast Asia caused by El Niño and worsened by global warming. *Nature Communications*, *8*(1), 15531. https://doi.org/10.1038/ncomms15531

Thompson, R. L., Chevallier, F., Crotwell, A. M., Dutton, G., Langenfelds, R. L., Prinn, R. G., et al. (2014). Nitrous oxide emissions 1999 to 2009 from a global atmospheric inversion. *Atmospheric Chemistry and Physics*, *14*(4), 1801–1817. https://doi.org/10.5194/acp-14-1801-2014

Tian, H., Xu, R., Canadell, J. G., Thompson, R. L., Winiwarter, W., Suntharalingam, P., et al. (2020). A comprehensive quantification of global nitrous oxide sources and sinks. *Nature*, *586*(7828), 248–256. https://doi.org/10.1038/s41586-020-2780-0

Tian, H., Yang, J., Lu, C., Xu, R., Canadell, J. G., Jackson, R. B., et al. (2018). The global N_2O model intercomparison project. *Bulletin of the American Meteorological Society*, *99*(6), 1231–1251. https://doi.org/10.1175/BAMS-D-17-0212.1

Tsuruta, A., Aalto, T., Backman, L., Hakkarainen, J., van der Laan-Luijkx, I. T., Krol, M. C., et al. (2017). Global methane emission estimates for 2000–2012 from Carbon-Tracker Europe-CH_4 v1.0. *Geoscientific Model Development*, *10*(3), 1261–1289. https://doi.org/10.5194/gmd-10-1261-2017

Vadrevu, K. P., Lasko, K., Giglio, L., Schroeder, W., Biswas, S., & Justice, C. (2019). Trends in vegetation fires in South and Southeast Asian countries. *Scientific Reports*, *9*(1), 7422. https://doi.org/10.1038/s41598-019-43940-x

Vancutsem, C., Achard, F., Pekel, J.-F., Vieilledent, G., Carboni, S., Simonetti, D., et al. (2021). Long-term (1990–2019) monitoring of forest cover changes in the humid tropics. *Science Advances*, *7*, 10. https://doi.org/10.1126/sciadv.abe1603

van der Laan-Luijkx, I. T., vander Velde, I. R., van der Veen, E., Tsuruta, A., Stanislawska, K., Babenhauserheide, A., et al. (2017). The CarbonTracker data assimilation shell (CTDAS) v1.0: Implementation and global carbon balance 2001–2015. *Geoscientific Model Development*, *10*(7), 2785–2800. https://doi.org/10.5194/gmd-10-2785-2017

van der Werf, G. R., Dempewolf, J., Trigg, S. N., Randerson, J. T., Kasibhatla, P. S., Giglio, L., et al. (2008). Climate regulation of fire emissions and deforestation in equatorial Asia. *Proceedings of the National Academy of Sciences of the United States of America*, *105*(51), 20350–20355. https://doi.org/10.1073/pnas.0803375105

van der Werf, G. R., Randerson, J. T., Giglio, L., van Leeuwen, T. T., Chen, Y., Rogers, B. M., et al. (2017). Global fire emissions estimates during 1997–2016. *Earth System Science Data*, *9*(2), 697–720. https://doi.org/10.5194/essd-9-697-2017

Wang, F., Maksyutov, S., Tsuruta, A., Janardanan, R., Ito, A., Sasakawa, M., et al. (2019). Methane emission estimates by the global high-resolution inverse model using national inventories. *Remote Sensing*, *11*(21), 2489. https://doi.org/10.3390/rs11212489

Wang, Y., Hollingsworth, P. M., Zhai, D., West, C. D., Green, J. M. H., Chen, H., et al. (2023). High-resolution maps show that rubber causes substantial deforestation. *Nature*, *623*(7986), 340–346. https://doi.org/10.1038/s41586-023-06642-z

Wells, K. C., Millet, D. B., Bousserez, N., Henze, D. K., Chaliyakunnel, S., Griffis, T. J., et al. (2015). Simulation of atmospheric N2O with GEOS-chem and its adjoint: Evaluation of observational constraints. *Geoscientific Model Development*, *8*(10), 3179–3198. https://doi.org/10.5194/gmd-8-3179-2015

Wetlands International. (2003). Maps of peatland distribution and carbon content in Sumatera (pp. 1990–2002).

Wetlands International. (2004). Maps of peatland distribution and carbon content in Kalimantan (pp. 2000–2002).

Wijedasa, L. S., Sloan, S., Page, S. E., Clements, G. R., Lupascu, M., & Evans, T. A. (2018). Carbon emissions from South-East Asian peatlands will increase despite emission-reduction schemes. *Global Change Biology*, *24*(10), 4598–4613. https://doi.org/10.1111/gcb.14340

Wilson, C., Chipperfield, M., Gloor, M., & Chevallier, F. (2014). Development of a variational flux inversion system (INVICAT v1. 0) using the TOMCAT chemical transport model. *Geoscientific Model Development*, *7*(5), 2485–2500. https://doi.org/10.5194/gmd-7-2485-2014

Xu, Y., Yu, L., Ciais, P., Li, W., Santoro, M., Yang, H., & Gong, P. (2022). Recent expansion of oil palm plantations into carbon-rich forests. *Nature Sustainability*, *5*, 574–577. https://doi.org/10.1038/s41893-022-00897-6

Yoshida, Y., Kikuchi, N., Morino, I., Uchino, O., Oshchepkov, S., Bril, A., et al. (2013). Improvement of the retrieval algorithm for GOSAT SWIR XCO_2 and XCH_4 and their validation using TCCON data. *Atmospheric Measurement Techniques*, *6*, 1533–1547. https://doi.org/10.5194/amt-6-1533-2013

Zeng, Z., Estes, L., Ziegler, A. D., Chen, A., Searchinger, T., Hua, F., et al. (2018). Highland cropland expansion and forest loss in Southeast Asia in the twenty-first century. *Nature Geoscience*, *11*(8), 556–562. https://doi.org/10.1038/s41561-018-0166-9

Zheng, B., Chevallier, F., Ciais, P., Yin, Y., Deeter, M. N., Worden, H. M., et al. (2018). Rapid decline in carbon monoxide emissions and export from East Asia between years 2005 and 2016. *Environmental Research Letters*, *13*(4), 044007. https://doi.org/10.1088/1748-9326/aab2b3

Zheng, B., Chevallier, F., Ciais, P., Yin, Y., & Wang, Y. (2018). On the role of the flaming to smoldering transition in the seasonal cycle of African fire emissions. *Geophysical Research Letters*, *45*(21), 11998–12007. https://doi.org/10.1029/2018GL079092

Zscheischler, J., Mahecha, M. D., Avitabile, V., Calle, L., Carvalhais, N., Ciais, P., et al. (2017). Reviews and syntheses: An empirical spatio-temporal description of the global surface–atmosphere carbon fluxes: Opportunities and data limitations. *Biogeosciences*, *14*(15), 3685–3703. https://doi.org/10.5194/bg-14-3685-2017

19449224, 2025, 9, Downloaded from https://agupubs.onlinelibrary.wiley.com/doi/10.1029/2024GB008256 by Indian Institute Of Tech - Roorkee, Wiley Online Library on [14/03/2026]. See the Terms and Conditions (https://onlinelibrary.wiley.com/terms-and-conditions) on Wiley Online Library for rules of use; OA articles are governed by the applicable Creative Commons License